

# **PDGF Gene Therapy to Accelerate Dental Implant Osseointegration**

By

**Qiming Jin DDS, Ph.D**

A thesis submitted in partial fulfillment  
of the requirements for the degree of Master of Science in  
Restorative Dentistry  
The University of Michigan  
2009

Horace A Rackham School of Graduate Studies  
University of Michigan  
Ann Arbor, MI  
2009

## **Thesis Committee:**

Professor William V. Giannobile-Chairman  
Professor Peter Yaman  
Professor Joseph D. Dennison

## **DEDICATION**

**To my beloved wife and son**

## ACKNOWLEDGMENTS

First of all, I would like to thank all people who have helped and inspired me during my restorative program study.

Especially, I would like to give my heartfelt thanks and deep gratitude to my supervisor, Professor William V. Giannobile, for his continuous support in my study, research and work. It would be impossible for me to finish my study without his generous help.

I am also heartily thankful to the rest of my thesis committee and my clinical supervisors: Professors Peter Yaman and Joseph D. Dennison, for their patience and tremendous efforts in helping me improve my clinical skills, which made my clinical practice such a rewarding time to me.

My sincere thanks also go to the members of Giannobile Lab: James V. Sugai, Po-Chun Chang, Joni A. Cirrelli, Yang-Jo Seol, Chan Ho Park, Zhao Lin for their contributions in this study. Particularly, I am obliged to Po-Chun Chang for his most input.

I am grateful to my clinical instructors and staff: Dr. Gisele Neiva, Dr. Jacques Nör, Dr. Jose Vivas, Dr. Kenneth Stoffers, Dr. Domenica Sweier, Dr. John Heys, Dr. Dennis Fasbinder, Dr. Mark Zahn, Bonnie Dawson, Nancy Damberg, Dana Baloh, Theresa Brown, Anja Buschhaus, Lisa Klave, Amy Lawson, Angela Reau, Kay Wall, for their great mentorship and general assistance.

Finally, I would like to give my warmest regards and blessings to all of those who have supported me in any respect during my restorative program study.

## TABLE OF CONTENTS

<b>DEDICATION</b>	ii
<b>ACKNOWLEDGEMENTS</b>	iii
<b>TABLE OF CONTENTS</b>	iv
<b>LISTS OF TABLES</b>	vi
<b>LISTS OF FIGURES</b>	vii
<b>INTRODUCTION and LITERATURE REVIEW</b>	1
Rationale for Dental Implant Application	1
Clinical Major Challenges for Dental Implant	2
Growth Factor Gene Therapy To Enhance Implant Osseointegration	2
PDGF Biological Functions and Its Gene Therapy	3
<b>SPECIFIC AIMS and HYPOTHESIS</b>	5
Specific Aim 1: To evaluate safety of PDGF gene local delivery approach.	5
Specific Aim 2: To determine the potential of PDGF gene delivery approach to regenerate alveolar bone around titanium implants in rats.	5
<b>EXPERIMENT DESIGN, MATERIALS and METHODS</b>	7
Experiment Design for Specific Aim 1	7
Adenovirus Vectors Preparation	7
Preparation of Adenovirus-Gene Activated Matrix.	7
Periodontal Alveolar Bone Wound Model and Ad/PDGF-B Treatment	8
Tissue Harvesting, Histological, and Histopathological Observations	8
Quantitative Polymerase Chain Reaction (qPCR) Assay.	9
Experiment Design for Specific Aim 2	10
Preparations of Recombinant Adenovirus Vectors and Delivery Matrix	11
Well-type Osteotomy Creation, Implant Placement and Treatments	11
BS-SEM, Histology and Histomorphometry	12

MicroCT 3-D Evaluations	13
Statistical Analysis	14
<b>RESULTS, DISCUSSIONS, and CONCLUSIONS</b>	<b>15</b>
A: Adenovirus Encoding Human Platelet-Derived Growth Factor-B Delivered to Alveolar Bone Defects Exhibits Safety and Biodistribution Profiles Favorable for Clinical Use (Chang et al. Hum Gene Ther. 2009 May;20(5):486-96.)	15
Results and Discussion	19-25
B: PDGF-B gene therapy accelerates bone engineering and oral implant osseointegration. (Chang et al. Gene Ther. 2009 (in press))	27
Results and Discussion	28-34
<b>REFERENCES</b>	<b>38</b>

## LIST OF TABLES

Table. Hematological analysis for Ad/PDGF-B delivery to alveolar bone defects	21
Table. Clinical chemistry analysis for Ad/PDGF-B delivery to alveolar bone defects	22
Table. Ad/PDGF-B qPCR results in bloodstream and distant organs	24
Table. Hematological analysis for Ad/PDGF-B delivery to dental implant sites	32
Table. Clinical chemistry analysis for Ad/PDGF-B delivery to dental implant sites	32

## LIST OF FIGURES

Figure. Dental implant osteotomy defect model for gene delivery	12
Figure. Study design and body weight change over time	18
Figure. PDGF gene delivery promotes periodontal tissue regeneration <i>in vivo</i>	20
Figure. Vector transduction efficiency and systemic distribution of bioluminescence	23
Figure. Histological view of each group for dental implant evaluations for 10 and 14 days.	29
Figure. Backscattered SEM images and two dimensional evaluations for dental implants	30
Figure. Biomechanical and microCT/functional stimulations show that Ad/PDGF-B and PDGF-BB improve osseointegration <i>in vivo</i>	31
Figure. Experimental design for dental implants and experimental model illustration	34

## INTRODUCTION

Dental implants are widely used to restore missing teeth or to serve as abutments for a bridge, partial dental or complete denture. It is reported that 69% of adults in the U.S. ages 35 to 44 have lost at least one permanent tooth due to trauma, periodontitis, a failed root canal, or tooth decay. By age 74, 26% of adults have lost all of their permanent teeth. (1) In 2008, the global dental implant market increased to \$3.4 billion dollars, while the market for traditional crowns and bridges decreased to \$4.4 billion dollars. The market value of dental implants is anticipated to reach \$8.1 billion by 2015. (1)

### **Rationale for Dental Implant Application**

Dental implants have many advantages over transitional crowns, bridges or dentures. Dental implants are able to preserve tooth structures, because there is no need to remove adjacent abutment teeth structures for a bridge. It is not necessary to consider the risk of recurrent caries in dental implants, while caries is considered to be the most frequent reason for failure of existing restorations such as onlays, crowns, and bridges. (2) Implants can provide much more stability and retention of implant supported prosthesis than traditional tooth/tissue -borne partial dentures and tissue borne complete dentures. (3) In addition, the most important aspect of dental implants is to preserve alveolar bone. Carlsson et al. have reported that marginal periimplant bone loss over a 10-year observation period was less than 1 mm for both mandible and maxillae. (4) However, the loss of alveolar bone after just 1 year following tooth extraction reached 6 mm in width and 1.2 in height. (5) Because of alveolar bone preservation, dental implants can be used to restore and maintain the gingival tissue emergence profile in the maxillary esthetic zone after anterior tooth extraction. (6) Furthermore, the property of the prevention of implants from alveolar bone loss may be a key rationale for its more than 90% long-term survival rate.

## **Major Clinical Challenges for Dental Implants**

Dental implants require sufficient alveolar bone, both in width and in length, to acquire adequate primary stability, and to eventually exert its support function. In some cases such as severely atrophic edentulous mandibles and thin maxillary sinus floor, without bone augmentation, implant treatment is not an option for patients with severe alveolar bone absorption. In addition, bone loss also results in some problems in the anterior maxilla for esthetic reasons. (6) On the other hand, patients with implant placement should wait 3 to 6 months clinically for successful osseointegration formation and final permanent restoration. Therefore, how to augment alveolar bone and shorten the clinical waiting time are two major clinical challenges for dental implantology.

## **Growth Factor Gene Therapy To Enhance Implant Osseointegration**

Traditional techniques for enhancing bone formation for dental implant placement include bone autografts, allografts or guided bone regeneration.(7) The use of osteogenic growth factors such as PDGF to regenerate tooth-supporting and peri-implant bone in preclinical animal models (8-12) and in early human trials (13, 14)has offered significant potential for periodontal regenerative medicine. However, outcomes of these therapies are limited in terms of regeneration and predictability. The utilization of gene therapy to control the release and bioavailability of osteogenic growth factors (GFs) offers potential for tissue engineering periodontal and peri-implant bone defects. (15)

Despite many of the positive results using growth factors for alveolar bone regeneration, drug instability at the site of delivery contributes to the need of pharmacologic dosing, which is limited by local and systemic toxicity. (16) The therapeutic delivery of growth factors requires a well-characterized delivery system to safely target the factors to the wound. A few human trials

using GFs reported to date have utilized superphysiological doses of GFs that result in “dose-dumping” of potent biologics in the wound site. (17-19) This use of bolus delivery can lead to systemic toxicity,(20) likely through cytokine diffusion into the bloodstream. (21) Although clinical trials have offered encouraging initial results, the degree of tooth-supporting tissue regeneration achieved from these studies is suboptimal. Systematic reviews of the literature of current periodontal therapies suggest these treatments result in only slight improvements in bone regeneration (usually <50% regeneration) and for horizontal defects (<20%) improvement. (22, 23) A possible reason for these minimal results may be related to the short half-life of biomolecules delivered to osseous tooth-supporting defects *in vivo*, as well as the minimal levels of bioactive factors that may be available in tissue banked bone. Our recent work in the area (see attached publications) demonstrates: 1. the potency of Ad/PDGF-B to stimulate tooth-supporting bone; (24) 2: Our ability to develop and utilize a model of dental implant osseointegration in small animals for gene therapy applications; (25) and 3: our ability to demonstrate safety (26) and has offered many significant advances using gene therapy to repair tooth-supporting defects. Therefore, gene transfer offers significant potential to improve growth factor delivery to dental implant-associated bone defects.

### **PDGF Biological Functions and Gene Therapy**

Platelet derived growth factor (PDGF) is a member of a multifunctional polypeptide family, which is composed of A, B, C and D polypeptide chains that form homo- or heterodimeric molecules.(27) PDGF binds to two structurally-related intrinsic tyrosine kinase receptors (PDGF-R $\alpha$  and PDGF-R $\beta$ ) and subsequently exerts its biological effects on cell migration, proliferation, extracellular matrix synthesis, and anti-apoptosis.(28-32) PDGF not only plays a crucial role in the development of the heart, kidney, and vasculature,(33) but also contributes to

tissue repair.(15) PDGF- $\alpha$  and - $\beta$  receptors are induced in regenerating periodontal soft and hard tissues.(34, 35) In addition, PDGF initiates tooth-supporting periodontal ligament (PDL) cell chemotaxis,(36) mitogenesis,(37) matrix synthesis,(38, 39) and attachment to tooth dentinal surfaces.(40) More importantly, *in vivo* application of PDGF alone or in combination with insulin-like growth factor-I (IGF-I) results in partial repair of periodontal tissues as shown in preclinical and clinical investigations.(10, 13, 41, 42) Recently, PDGF is FDA-approved for the treatment of neurotrophic diabetic ulcers(43) and for promoting bone repair of periodontal osseous defects, (44, 45) indicating that PDGF has an important impact not only on soft tissues, but also on osseous tissues. PDGF gene transfer has been shown to stimulate gingival fibroblast, PDL and tooth-lining cell (cementoblast) mitogenesis and proliferation above that of continuous PDGF administration *in vitro*.(46, 47) Adenovirus-mediated PDGF-B gene transfer accelerates gingival soft tissue wound healing in an *ex vivo* wound repair model.(48) Therefore, we will explore in this study the significant potential of adenovirus-mediated PDGF-B gene transfer to improve bone regeneration at rat dental implant-associated bone defects.

## **SPECIFIC AIMS and HYPOTHESIS**

**Specific Aim 1: To evaluate safety of PDGF gene local delivery approach.** Hypothesis: the controlled local delivery of PDGF-B gene by recombinant adenovirus vectors will be localized without distant organ involvement. Safety of any clinical approaches is the first consideration. Periodontal alveolar bone defects were created in rat mandibles, and recombinant adenoviruses encoding PDGF-B with collagen carrier were added into the defects. Collagen carrier alone was used as a negative control. At designated time points during 3-35 days postdelivery, rats were sacrificed, and tissue in the defects and many organs were harvested. DNA in tissues and organs were extracted. The biodistribution of PDGF adenovirus vectors were evaluated by real-time PCR. In addition, the changes of tissues and organs after PDGF gene delivery were observed histologically.

**Specific Aim 2: To determine the potential of PDGF gene delivery approach to regenerate alveolar bone around titanium implants in rats.** Hypothesis: The controlled delivery of growth factor genes will stimulate new bone formation in the defects around dental implants. Large osteotomy bone defects were created in rats following tooth extraction and treated with recombinant adenoviruses encoding PDGF-B, or human recombinant PDGF-BB, or collagen carrier alone. Simultaneous with gene delivery, endosseous dental implants were placed. The kinetics and extent of bone volume achieved adjacent to the dental implants were measured using microCT, back-scattered EM, and conventional histomorphometric analysis.

Results from these studies will aid in the better understanding of the role of sustained growth factor gene delivery on peri-implant wound repair. The long-term goal of this project will optimize and validate gene therapeutic approaches to provide sufficient evidence to consider the development of

a pivotal study using PDGF gene delivery to promote bone regeneration of dental implant defects in humans.

# EXPERIMENT DESIGN, MATERIALS, and METHODS

## Experiment Design for Specific Aim 1

In order to investigate the biodistribution of PDGF adenovirus vectors after local delivery, periodontal osseous defects were created at the mandibles of a total of 144 (75 male, and 69 female) 10-week old Sprague-Dawley rats (weighing 250-300 grams). These defects were treated with Ad/PDGF-B at  $5.5 \times 10^8$  pfu/ml (low-dose), Ad/PDGF-B at  $5.5 \times 10^9$  pfu/ml (high-dose), and collagen matrix alone, respectively. At day 1, 2, 3, 4, 5, 7, 14, 21, 28, and 35 after surgery, the rats were sacrificed. Tissue in defects, blood, the submandibular lymph nodes, axillary lymph nodes, brain, lung, heart, liver, spleen, kidney, and testes from male rats, as well as ovaries from female rats were harvested. One part of the tissues and organs was used to extract DNA. The biodistribution of PDGF adenovirus vectors were evaluated by real-time PCR. The other was used to prepare histology routine sections.

## Adenovirus Vectors Preparation

E1-, E3-deleted human adenovirus serotype 5 vectors encoding human platelet-derived growth factor-B (Ad/PDGF-B) under control of the cytomegalovirus promoter were employed in this study. Titers of virus stocks were determined on embryonic kidney 293 cells by plaque assay and expressed as the plaque-forming units (pfu) per milliliter. Two different doses of adenoviral vectors were examined in this study,  $5.5 \times 10^8$  pfu/ml and  $5.5 \times 10^9$  pfu/ml. These dose levels were equivalent to Ad-PDGFB concentrations previously described.(24)

## Preparation of Adenovirus-Gene Activated Matrix.

Ad-PDGF-B were dialyzed into GTS buffer (2.5% glycerol, 25 mM NaCl, 20 mM Tris, pH 8.0) and formulated in bovine fibrillar type I collagen matrix (Matrix Pharmaceutical Inc., Fremont, CA, USA) at a final concentration of 2.6%.

## **Periodontal Alveolar Bone Wound Model and Ad/PDGF-B Treatment**

All animal experiments were approved by the University of Michigan Institutional Animal Care and Use Committee. A total of 144 (75 male, and 69 female) 10-week old Sprague-Dawley rats (weighing 250-300 grams) were utilized in this study. Three different adenovirus-gene activated matrices were prepared immediately prior to surgery, containing  $5.5 \times 10^8$  pfu/ml (low-dose),  $5.5 \times 10^9$  pfu/ml (high-dose) of AdPDGF-B, and collagen matrix alone. For surgical operations, the animals were anesthetized with ketamine (50 mg/kg) and xylazine (10 mg/kg), followed by analgesia as needed with buprenex (0.1-0.5 mg/kg, Reckitt Benckiser Healthcare Ltd., Hull, England). A standardized 3 x 2 x 1 mm osseous defect was created in the buccal plate overlying the mandibular first molar and second molar tooth roots as previously described (49). The exposed roots were carefully denuded of periodontal ligament, cementum, and superficial dentin. Then 20 $\mu$ l of adenovirus/collagen matrix were delivered to the defects, filling them to entirety. The wounds were closed by suturing the superficial musculature layers and approximating the skin by surgical clips. The rats received analgesics on the following day as needed for up to 7 days post-surgery. The animals also received supplemental antibiotics (ampicillin 268 mg/L of dextrose in distilled water) for 7 days. The surgical clips were removed 10 days following surgery.

## **Tissue Harvesting, Histological, and Histopathological Observations**

Upon sacrifice at designated time points, the submandibular lymph nodes, axillary lymph nodes, brain, lung, heart, liver, spleen, kidney, and testes from male rats, and the entire tissue within defect area as well as ovaries from female rats were harvested. The ipsilateral organs were chosen, and for organs with abundant DNA (heart, lung, liver, spleen, kidney, sex organs, and brain), sectioning was done at the center of each specimen. Half of the selected tissues were then preserved in a -80°C freezer for DNA extraction, and the remaining half were fixed with 10%

formalin for 24 hours and transferred to 75% ethanol for subsequent histological and histopathological analysis. The defect mandibulae were decalcified with 10% acetic acid, 4% formaldehyde, and 0.85% NaCl for 3 weeks. Then, decalcified mandibulae and the organ specimens were dehydrated in step gradients of ethanol and embedded in paraffin. Sections from two different regions (border and central level of defect) were made in mandibular samples and 3-6 slices from the central-cut sections (5-8 mm in thickness). Hematoxylin and eosin staining was performed on all histological sections followed by pathological examination. A thorough histopathological examination was performed for all sections.

### **Quantitative Polymerase Chain Reaction (qPCR) Assay.**

Quantitative TaqMan PCR was used to determine the vector copy number of AdPDGF-B in the bloodstream and organs. The primers used for quantitative real time PCR (QPCR) bridging the vector backbone and PDGF-BB prepro region were: sense -- 5'-GGATCTTCGAGTCGACAAGCTT-3'; anti-sense --5'-ATCTCATAAAGCTCCTCGGGAAT-3'; internal fluorogenic probe -- 5'-CGCCCAGCAGCGATTCATGGTGAT-3'. QPCR was performed by using TaqMan Universal PCR Master Mix (Applied Biosystems). Briefly, a 30 µl PCR reaction was prepared with 500 ng DNA and 1.5µl mixture of gene fluorogenic probe and primers. The thermal conditions were: 50°C 2 min, 95°C 10 min followed by 45 cycles of 95°C, 15 sec and 60°C, 1 min, and the resulting amplicon was detected by ABI Prism 7700 sequence detection instrument (Applied Biosystems). The standard curve was determined by using a range of 10<sup>1</sup> to 10<sup>5</sup> AdPDGF-B particles (regression correlation coefficient > 95%). The possibility of cross-reactivity was evaluated by adding adenoviral vector encoding PDGF-A, PDGF-1308 (dominant-negative mutant PDGF), bone morphogenetic protein-7, noggin, bone sialoprotein, Luciferase, and GFP for

comparison. No enhancement or inhibition of signal was noted when tissues were spiked with these vectors.

For blood DNA, the samples were collected from 6 rats per gender in the four groups (high-dose AdPDGF-B, low-dose AdPDGF-B, collagen matrix only, and no treatment) prior to surgery, and throughout 35 days after gene delivery. 50  $\mu$ l whole blood was isolated and DNA was obtained by QIAamp DNA blood Mini kit (QIAGEN Inc., Valencia, CA, USA). For organ and tissue DNA, the total tissue in the defect area and surrounding musculature, submandibular lymph node, axillary lymph nodes, brain, lung, heart, liver, kidney, spleen, and sex organs (testes and ovaries) were excised from 3 rats in each of the three groups (high-dose AdPDGF-B, low-dose AdPDGF-B, and collagen matrix only) post-sacrifice, and triplicate experiments were performed. The time points analyzed were from 3 to 35 days. Each PCR reaction contained 500 ng test DNA without spiking. Pre-study experiments demonstrated expected signal enhancement using AdPDGF-B spiking (500 copies per reaction, *data not shown*). The limitation of detection was 30 copies per 500 ng test DNA for all the specimens.

### **Experiment Design for Specific Aim 2**

In order to evaluate the effects of PDGF gene delivery approach on dental implant osseointegration, a total of 82 male Sprague-Dawley rats were used. Based on the power analysis calculations from a previous similar study, 6-8 animals were required per treatment per time point. (24) Four weeks after the maxillary first molar were extracted bilaterally, a well-type osteotomy was created. Following implant placement, four treatments were performed:  $.5 \times 10^9$  pfu/ml Ad-Luc as a negative control,  $5.5 \times 10^8$  pfu/ml Ad/PDGF-B,  $5.5 \times 10^9$  pfu/ml Ad/PDGF-B, or 0.3 mg/ml rhPDGF-BB as a positive control. At day 10, 14 and 21 after implantation, the maxillae

containing implant were harvested, examined by microCT, BS-SEM, histology and histomorphometry.

### **Preparations of Recombinant Adenovirus Vectors and Delivery Matrix**

Please see the above.

### **Well-type Osteotomy Creation, Implant Placement and Treatments**

All animal procedures followed the guidelines from the Committee on Use and Care of Animals of the University of Michigan. The maxillary first molars were extracted bilaterally 4 weeks prior to dental implant installation. After healing, an osteotomy was created using a custom drill-bit. The drill-bit was designed with a 0.95 mm diameter, 1 mm long-apical portion and a 2.2 mm diameter, 1 mm long at the coronal aspect. The apical part of the drill created an osteotomy for initial fixation and the coronal part of the drill created a circumferential osseous defect prior to dental implant installation. A custom cylinder-type titanium mini-implant (gift of Institut Straumann AG, Basel, Switzerland), 1 mm-in-diameter and 2 mm-in-depth, was press-fit into the surgically-created socket( Fig 1. A). The remaining defect was then filled with the type I collagen matrix containing  $5.5 \times 10^9$  pfu/ml Ad-Luc,  $5.5 \times 10^8$  pfu/ml Ad-PDGF-B,  $5.5 \times 10^9$  pfu/ml Ad-PDGF-B, or 0.3 mg/ml rhPDGF-BB (Fig1. B). Ad-Luc has not previously exhibited biological activities in dentoalveolar defects (24)and served as control group in this study. The surgical area was covered by gingival tissue and closed using butyl cyanoacrylate (Periacryl<sup>®</sup>, Glustitch Inc., Point Roberts, WA, USA). The vital fluorochrome dye, calcein (10 mg/kg), was injected intra-muscularly after 3 days, and antibiotics (268 mg/L ampicillin in 5% dextrose water) were provided in the first 7 days post-operation.

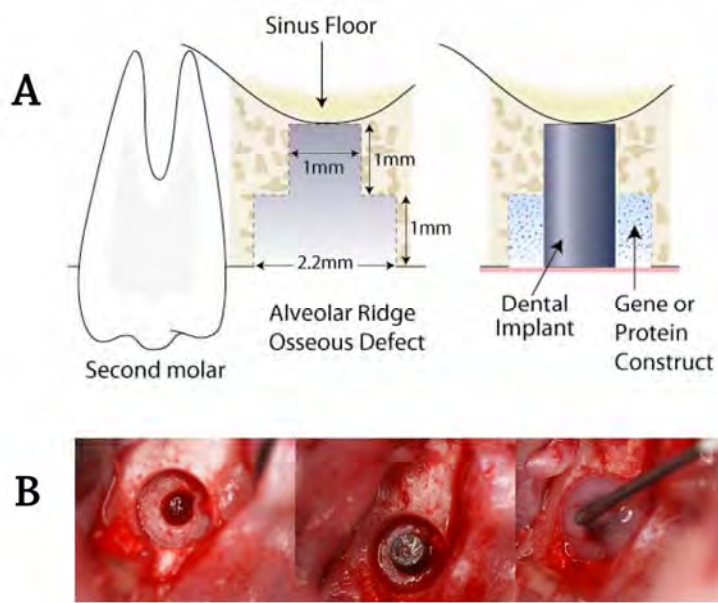


**Fig 1.** A. Dental Implant Osteotomy Defect Model for Gene Delivery. “Well-type” osteotomy defects were created that measured 1 mm in depth and 2 mm coronally (left panel). The titanium dental implant was press fit into position (middle panel), followed by the delivery of the 2.6% collagen matrix containing either Ad/PDGF-B or collagen gel alone (right panel). B. High magnification photos from the surgical operation corresponding to 1A taken at 10x magnification including defect creation (left panel), dental implant placement (middle) and gene delivery (right).

### **BS-SEM, Histology and Histomorphometry**

Maxillae containing the implants were harvested upon sacrifice, with one side of maxillae taken for backscattered SEM and histology while the contralateral maxillae were used for microCT after removing implant to avoid metal scattering influence. The specimens were fixed in 50% ethanol for at least 72 hours and subsequently embedded in epoxy resin. The specimens were then sectioned in the longitudinal direction relative to the implants using a diamond saw blade (Crystalite Co., Westerville OH, USA), then polished to achieve a 50-100  $\mu\text{m}$  final thickness. The tissue mineralization was evaluated under the backscattered mode on Qanta F1B SEM with 45x

magnification, calibrated with aluminum and carbon discs (50), and transferred to physical density using bone substitute radiographic phantoms (Gammex Inc., Middleton WI, USA). The photographs were then segmented and thresholded by Otsu's adaptive technique (51). To eliminate any metal scattering effect, the measured bone-implant interface was defined as the horizontal distance 5 $\mu\text{m}$  from the outermost homogenous high-intensity area. The defect borders were projected using the calcein fluorescent images. Bone-area fractions (BAF, the ratio of newly-formed bone in the defect to the entire defect area) and Tissue mineral density within the defect (TMD, the average grayscale level of mineralized tissue within the defect area) were measured from backscattered SEM images. Next, histologic staining by methylene blue was performed, with the acid fuchsin utilized as the counterstaining. Bone-implant contact (BIC, the ratio of the length of bone contacting the titanium to the entire length of titanium interface with the defect area) and defect fill (DF, the ratio of bone-occupied area to the entire defect area) were measured.

### **MicroCT 3-D Evaluations**

After implant removal, micro-CT scans were performed using an eXplore Locus SP Micro-CT system (GE HealthCare, London, ON, Canada) and reconstructed to voxel size of 18x18x18  $\mu\text{m}^3$ . The spatial relationship of the mini-implant and surrounding tissues was then analyzed using a customized MATLAB<sup>®</sup> (Mathworks Inc., Natick, MA, USA) algorithm. The images were segmented with a threshold determined by Otsu's adaptive technique (51), and several parameters were quantitatively evaluated within the osseous defect areas: (1) Bone volume fraction (BVF): the volume of mineralized tissue within the osseous wound divided by the volume of osseous wound; (2) Tissue mineral density (TMD): the mineral content of the radiographic-defined mineralized tissue within the osseous wound divided by the volume of

osseous wound; (3) Bone mineral density (BMD): the mineral density within the radiographic-defined mineralized tissue in the osseous wound.

### **Statistical Analysis**

One way ANOVA with Tukey post hoc test was used to analyze the difference of parameter data obtained from histomorphometry performed on BS-SEM photos or MicroCT 3-D images of biopsies at each groups. The statistical difference was considered with a p-value of < 0.05.

## **RESULTS, DISCUSSIONS, and CONCLUSIONS**

A: Adenovirus Encoding Human Platelet-Derived Growth Factor-B Delivered to Alveolar Bone Defects Exhibits Safety and Biodistribution Profiles Favorable for Clinical Use (Chang et al. Hum Gene Ther. 2009 May;20(5):486-96.)

Results and Discussion are on pages 19 ~ 25.

# Adenovirus Encoding Human Platelet-Derived Growth Factor-B Delivered to Alveolar Bone Defects Exhibits Safety and Biodistribution Profiles Favorable for Clinical Use

Po-Chun Chang,<sup>1,2</sup> Joni A. Cirelli,<sup>1</sup> Qiming Jin,<sup>1</sup> Yang-Jo Seol,<sup>1,3</sup> James V. Sugai,<sup>1</sup> Nisha J. D'Silva,<sup>1</sup> Theodora E. Danciu,<sup>1</sup> Lois A. Chandler,<sup>4</sup> Barbara A. Sosnowski,<sup>4</sup> and William V. Giannobile<sup>1,2</sup>

## Abstract

Platelet-derived growth factor (PDGF) gene therapy offers promise for tissue engineering of tooth-supporting alveolar bone defects. To date, limited information exists regarding the safety profile and systemic biodistribution of PDGF gene therapy vectors when delivered locally to periodontal osseous defects. The aim of this preclinical study was to determine the safety profile of adenovirus encoding the PDGF-B gene (AdPDGF-B) delivered in a collagen matrix to periodontal lesions. Standardized alveolar bone defects were created in rats, followed by delivery of matrix alone or containing AdPDGF-B at  $5.5 \times 10^8$  or  $5.5 \times 10^9$  plaque-forming units/ml. The regenerative response was confirmed histologically. Gross clinical observations, hematology, and blood chemistries were monitored to evaluate systemic involvement. Bioluminescence and quantitative polymerase chain reaction were used to assess vector biodistribution. No significant histopathological changes were noted during the investigation. Minor alterations in specific hematological and blood chemistries were seen; however, most parameters were within the normal range for all groups. Bioluminescence analysis revealed vector distribution at the axillary lymph nodes during the first 2 weeks with subsequent return to baseline levels. AdPDGF-B was well contained within the localized osseous defect area without viremia or distant organ involvement. These results indicate that AdPDGF-B delivered in a collagen matrix exhibits acceptable safety profiles for possible use in human clinical studies.

## Introduction

**P**LATELET-DERIVED GROWTH FACTOR (PDGF), a member of a multifunctional polypeptide family, is composed of disulfide-bonded A, B, C, or D polypeptide chains to form a homo- or heterodimeric molecule (Andrae *et al.*, 2008). PDGF is highly expressed in inflammatory cells, damaged bone, platelets, and mesenchymal cells (Southwood *et al.*, 2004). PDGF mediates mitogenesis and chemotaxis of mesenchymal cells and osteoblasts through tyrosine-phosphorylated signaling pathways (Ronnstrand and Heldin, 2001; Fiedler *et al.*, 2004). In oral tissues, PDGF also facilitates chemotaxis, matrix deposition, and attachment of periodontal ligament cells (Nishimura and Terranova, 1996; Haase *et al.*, 1998). Delivery of PDGF-BB has also demonstrated enhancement of periodontal wound repair (Cooke *et al.*, 2006) and re-

generation preclinically (Giannobile *et al.*, 1994, 1996; Park *et al.*, 2000) and in humans (Howell *et al.*, 1997; Nevins *et al.*, 2005).

Although exogenous growth factors improve the soft and hard tissue healing response, more sophisticated delivery methods are necessary to ensure adequate protein concentration and specific cell targeting to defect sites (Ramseier *et al.*, 2006; Cotrim and Baum, 2008). Recombinant adenoviruses (Ads) have been used as gene delivery vectors because of several unique features: (1) Ads have high transduction efficiency in both dividing and nondividing cells; (2) Ads do not induce apparent phenotypic changes in transduced cells; and (3) Ads do not integrate into the host genome and remain episomal (Gu *et al.*, 2004). Compared with recombinant growth factors, adenovirus encoding PDGF gene sequences (AdPDGF) can successfully transduce cells, prolong growth

<sup>1</sup>Department of Periodontics and Oral Medicine, School of Dentistry, University of Michigan, Ann Arbor, MI 48109.

<sup>2</sup>Department of Biomedical Engineering, College of Engineering, University of Michigan, Ann Arbor, MI 48109.

<sup>3</sup>Department of Periodontology, School of Dentistry, Seoul National University, Seoul 110-749, South Korea.

<sup>4</sup>Tissue Repair Co., San Diego, CA 92121.

factor expression, and induce downstream signaling pathways (Chen and Giannobile, 2002).

Adenoviral vectors administered to the head and neck for salivary gland repair have been previously studied and are now in clinical development (Cotrim *et al.*, 2007; Voutetakis *et al.*, 2008). Matrix-mediated delivery of DNA vectors has the potential to localize the vector and transgene products within the immediate delivery site (Chandler *et al.*, 2000). We have previously shown that AdPDGF-B delivery in collagen significantly improves cementogenesis and osteogenesis *in vivo* (Jin *et al.*, 2004). A preclinical investigation using the AdPDGF-B/collagen combination in a rabbit dermal wound model revealed robust localized wound healing responses with minimal systemic vector dissemination (Gu *et al.*, 2004).

On the basis of our current knowledge, no existing data describe the systemic effects of adenoviral vector delivered to the osseous craniofacial complex. In this study we sought to evaluate the safety profile for the local, collagen matrix-mediated delivery of AdPDGF-B for the promotion of alveolar bone healing. Vector copy number and expression at the defect site and various organs were quantified, and systemic hematology and blood chemistry were evaluated. In combination with histological findings, the data in the present study further support the clinical development of matrix-enabled gene therapy for periodontal wound regeneration.

## Materials and Methods

### Adenoviral vectors

E1-,E3-deleted human adenovirus serotype 5 vectors encoding transgenes under the control of the cytomegalovirus promoter were employed in this study. Adenovirus encoding human platelet-derived growth factor-B (AdPDGF-B) and adenovirus encoding firefly luciferase (AdLuc) were used for gene transfer. Titters of viral stocks were determined on embryonic kidney 293 cells by plaque assay and expressed as plaque-forming units (PFU) per milliliter. Two different doses of adenoviral vectors were examined in this study:  $5.5 \times 10^8$  and  $5.5 \times 10^9$  PFU/ml in 20  $\mu$ l of collagen matrix. These dose levels were equivalent to AdPDGF-B concentrations previously described (Jin *et al.*, 2004).

### Preparation of adenovirus gene-activated matrix

AdPDGF-B and AdLuc were dialyzed into GTS buffer (2.5% glycerol, 25 mM NaCl, 20 mM Tris; pH 8.0) and formulated in bovine fibrillar type I collagen matrix (Matrix Pharmaceutical, Fremont, CA) to a final concentration of 2.6%.

### Periodontal alveolar bone wound model and AdPDGF-B treatment

All animal experiments were approved by the Institutional Animal Care and Use Committee of the University of Michigan (Ann Arbor, MI). A total of 144 (75 male, and 69 female) 10-week-old Sprague-Dawley rats (weighing 250–300 g) were used in this investigation. The general timeline, grouping criteria, and study design are shown in Fig. 1A and total gender distributions for each experiment are described separately.

Two different adenovirus gene-activated matrices were prepared immediately before surgery, containing AdPDGF-B at  $5.5 \times 10^8$  PFU/ml (low dose), AdPDGF-B at  $5.5 \times 10^9$  PFU/ml (high dose), or collagen matrix alone. For surgical operations,

the animals were anesthetized with ketamine (50 mg/kg) and xylazine (10 mg/kg), followed by analgesia as needed with buprenorphine (Buprenex, 0.1–0.5 mg/kg; Reckitt Benckiser Healthcare, Hull, UK). Standardized  $3 \times 2 \times 1$  mm osseous defects were created in the buccal plate overlying the mandibular first molar and second molar tooth roots as previously described (Jin *et al.*, 2003). The exposed roots were carefully denuded of periodontal ligament, cementum, and superficial dentin. Twenty microliters of adenovirus/collagen matrix was then delivered to the defects, filling them to entirety. The wounds were closed by suturing the superficial musculature layers and approximating the skin by surgical clips. The rats received analgesics on the next day as needed for up to 7 days postsurgery. The animals also received supplemental antibiotics (ampicillin, 268  $\mu$ g/liter of dextrose in distilled water) for 7 days. The surgical clips were removed 10 days after surgery. Six rats without any surgical interventions (no treatment) were also included to compare the effect on body homeostasis of the surgical procedure versus no treatment.

### Body weight and clinical observations

Twenty-four male rats were distributed equally to four groups (high-dose AdPDGF-B, low-dose AdPDGF-B, collagen matrix only, and no treatment). The body weight of those animals was measured during the first 3 weeks. Clinical observation was focused on evaluation of the gross signs of swelling and lesions on days 3–35 as noted in Fig. 1A.

### Tissue harvesting, and histological and histopathological observations

On sacrifice, the submandibular lymph nodes, axillary lymph nodes, brain, lung, heart, liver, spleen, kidney, and testes (from male rats), and the entire tissue within defect area as well as ovaries (from female rats), were harvested with sterile scissors for each of the specific tissues and organs. The instruments were sterilized between tissue harvests, using a glass bead sterilizer. The ipsilateral organs were chosen, and for organs with abundant DNA (heart, lung, liver, spleen, kidney, sex organs, and brain), sectioning was done at the center of each specimen. Half of the selected tissues were then preserved in a  $-80^\circ\text{C}$  freezer for DNA extraction, and the remaining half were fixed with 10% formalin for 24 hr and transferred to 75% ethanol for subsequent histological and histopathological analysis. The defect mandibulae were decalcified with 10% acetic acid, 4% formaldehyde, and 0.85% NaCl for 3 weeks. Decalcified mandibulae and the organ specimens were then dehydrated in step gradients of ethanol and embedded in paraffin. Sections from two different regions (border and central level of defect) were made in mandibular samples and three to six slices from the central-cut sections ( $5\text{--}8 \mu\text{m}$  in thickness). Hematoxylin and eosin staining was performed on all histological sections, followed by pathological examination. The time points for analyses were from days 3 to 35 as described in Fig. 1A. A thorough histopathological examination was performed for all sections.

### Kinetics of luciferase expression by AdLuc/GAM *in vivo*

Adenovirus encoding luciferase (AdLuc) was formulated at concentrations of  $5.5 \times 10^8$  PFU/ml (low dose,  $n=6$ , 3 per

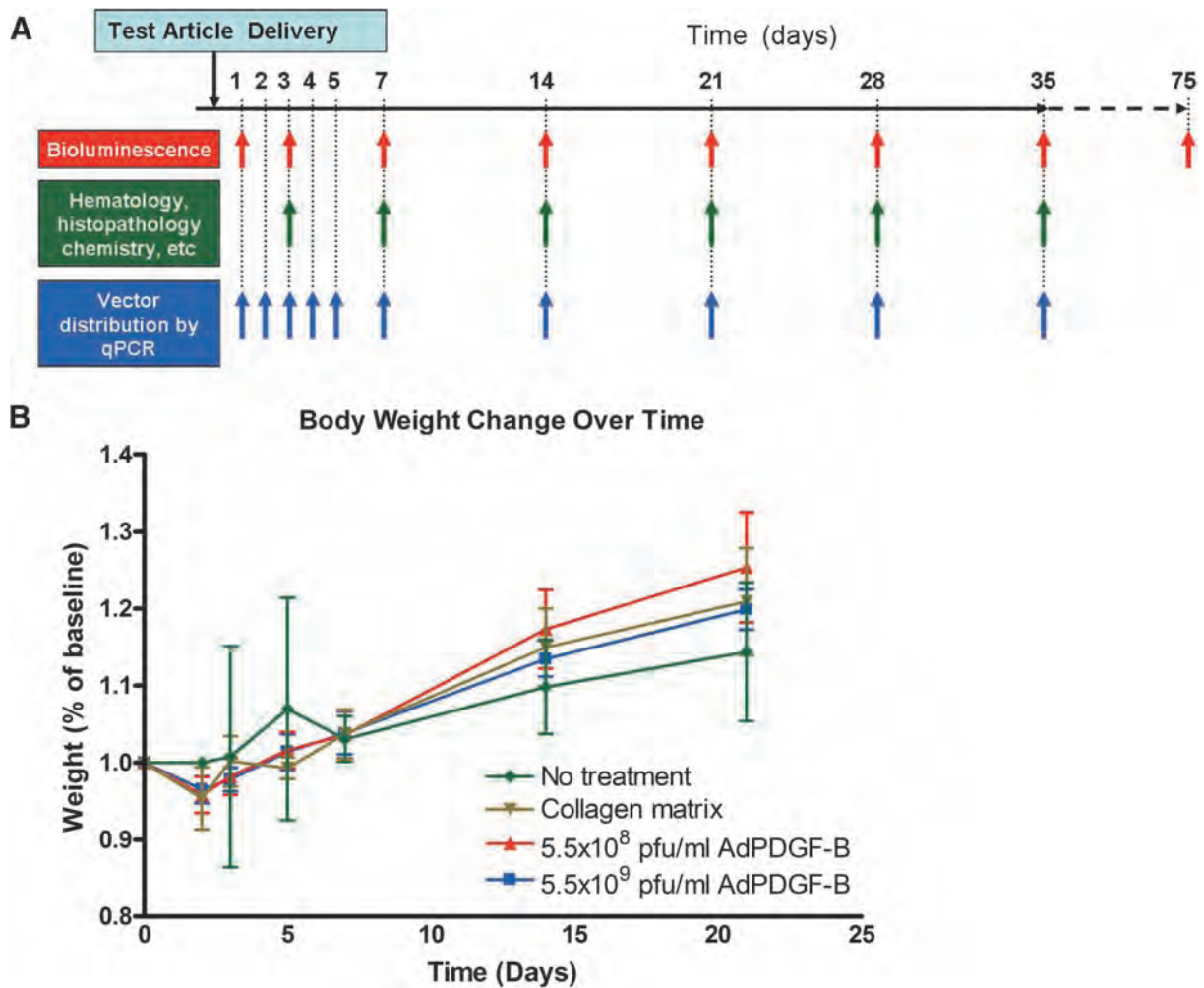


**FIG. 1.** General study design and body weight change over time. (A) Five treatment groups ( $5.5 \times 10^8$  PFU/ml AdLuc/collagen,  $5.5 \times 10^9$  PFU/ml AdLuc/collagen,  $5.5 \times 10^8$  PFU/ml AdPDGF-B/collagen,  $5.5 \times 10^9$  PFU/ml AdPDGF-B/collagen, and collagen matrix only) were investigated. The observation time points were over a period of 35 days on a weekly basis; two animals in  $5.5 \times 10^9$  PFU/ml AdLuc/collagen group were observed for 75 days. Nontreated animals (neither surgical defect nor adenovirus–collagen mixture application) were also included in the experiment to evaluate systemic involvement. (B) All the surgically treated animals experienced transient body weight loss in the first few days posttreatment but thereafter gained weight continuously throughout the study period.

gender) and  $5.5 \times 10^9$  PFU/ml (high dose,  $n = 6$ , 3 per gender) in  $20 \mu\text{l}$  of collagen matrix. Luciferase expression within each of the animals was measured with an *in vivo* imaging system (Xenogen/Caliper Life Sciences, Alameda, CA). To standardize the images, the cutoff threshold was set at  $5000 \text{ p/sec/cm}^2/\text{sr}$  to reduce the background signals, and the yield threshold was set at  $13,000 \text{ p/sec/cm}^2/\text{sr}$ . The amplitude of luciferase expression was calculated by subtracting the intensity of luciferin signal before and 12–15 min after luciferin (Promega, Madison, WI) injection (4 mg of luciferin per 25 g of body weight). The time points for evaluation are described in Fig. 1A.

#### Hematology and blood chemistry

All procedures were performed by the animal health diagnostic laboratory in the Unit for Laboratory Animal Medicine (ULAM) at the University of Michigan. Twenty-four male rats were distributed equally into four groups (high-dose

AdPDGF-B, low-dose AdPDGF-B, collagen alone, and no treatment), and blood was drawn from the day before surgery through 35 days postoperation (Fig. 1A). Fifty microliters of whole blood from each rat was placed into a tube containing EDTA anticoagulant for hematological specimens and a complete blood cell count (CBC) with automatic differential was performed. Serum ( $200 \mu\text{l}$ ) was drawn from each animal and the chemical parameters examined included alkaline phosphatase, calcium, phosphorus, creatinine kinase, albumin, globulin, total protein, blood urea nitrogen (BUN), creatinine, aspartate transaminase (AST), alanine transaminase (ALT), bilirubin, total bilirubin (T. bilirubin), amylase, glucose, and cholesterol.

#### Quantitative polymerase chain reaction assay

Quantitative TaqMan polymerase chain reaction (PCR) was used to determine the vector copy number of AdPDGF-B in the bloodstream and organs. The primers used for

quantitative real-time PCR (qPCR) bridging the vector backbone and PDGF-B prepro region were as follows: sense, 5'-GGATCTTCGAGTCGACAAGCTT-3'; antisense, 5'-ATCTCATAAAGCTCCTCGGAAT-3'; internal fluorogenic probe, 5'-CGCCCAGCAGCGATTGATGAT-3'. qPCR was performed with TaqMan universal PCR master mix (Applied Biosystems, Foster City, CA). Briefly, a 30- $\mu$ l PCR was prepared with 500 ng of DNA and a 1.5- $\mu$ l mixture of gene fluorogenic probe and primers. The thermal conditions were as follows: 50°C for 2 min, 95°C for 10 min, followed by 45 cycles of 95°C for 15 sec and 60°C for 1 min, and the resulting amplicon was detected with an ABI PRISM 7700 sequence detection instrument (Applied Biosystems). The standard curve was determined with a range of  $10^1$  to  $10^5$  AdPDGF-B particles (regression correlation coefficient, >95%). The possibility of cross-reactivity was evaluated by adding adenoviral vector encoding PDGF-A, PDGF-1308 (dominant-negative mutant PDGF), bone morphogenetic protein-7, noggin, bone sialoprotein, luciferase, and green fluorescent protein (GFP) for comparison. No enhancement or inhibition of signal was noted when tissues were spiked with these vectors.

For blood DNA, the samples were collected from 6 rats per gender (total of 12 per group) in the four groups (high-dose AdPDGF-B, low-dose AdPDGF-B, collagen matrix only, and no treatment) before surgery, and throughout 35 days after gene delivery (Fig. 1A). Fifty microliters of whole blood was isolated and DNA was obtained with a QIAamp DNA blood mini kit (Qiagen, Valencia, CA). For organ and tissue DNA, total tissue in the defect area and surrounding musculature, submandibular lymph node, axillary lymph nodes, brain, lung, heart, liver, kidney, spleen, and sex organs (testes and ovaries) was excised from three rats in each of the three groups (high-dose AdPDGF-B, low-dose AdPDGF-B, and collagen matrix only) postsacrifice, and triplicate experiments were performed. The time points analyzed were from 3 to 35 days (Fig. 1A). Each PCR contained 500 ng of test DNA without spiking. Prestudy experiments demonstrated expected signal enhancement with AdPDGF-B spiking (500 copies per reaction; data not shown). The limit of detection was 30 copies per 500 ng of test DNA for all the specimens.

#### Statistical analysis

Analysis of variance (ANOVA) was used to evaluate the differences in body weights and hematological and chemical parameters between experimental and control groups. Test groups were evaluated for time-dependent dynamics with collagen and nonsurgical groups, using Bonferroni posttests, and the significance was assessed by repeated-measures ANOVA. Results are presented as the mean  $\pm$  SD of measurements, with a *p* value less than 0.05 being considered statistically significant.

## Results

#### Clinical observations and body weight

All animals survived throughout the entire experimental period and among all surgically treated animals, no significant adverse events were noted beyond local swelling at the treatment sites, presumably caused by the surgical procedures. Body weight changes were normalized, using day 0 as

baseline, and the measures of weight change were evaluated as fractions relative to baseline weight. Results showed that after surgical treatment, all animals experienced slight weight loss within the first 2 days; however, they consistently gained weight over the course of the study. No significant weight changes were found among the three surgical groups at any time point (Fig. 1B).

#### Histology and histopathology

Two weeks after surgery, early bone formation could be observed within the defect area (Fig. 2A, top). Nearly complete bone bridging of the alveolar bone wounds was noted in both AdPDGF-B-treated groups, whereas there was limited bridging in the collagen-only animals. Cementogenesis could be seen in both AdPDGF-B-treated groups at 2 weeks but not in the collagen matrix group, and the defects treated with high-dose ( $5.5 \times 10^9$  PFU/ml) AdPDGF-B revealed more cementum formation compared with the other groups (Fig. 2A, bottom). At 35 days, the bone had completely bridged all of the defect area, and the fractions of defect fill became consistent in all animals. Animals receiving high-dose AdPDGF-B demonstrated greater evidence of cementogenesis along the tooth root (Fig. 2B).

Macroscopic evaluations of the harvested organs revealed no meaningful changes except mild enlargement of the submandibular lymph nodes in AdPDGF-B-treated (both high-dose and low-dose) and collagen matrix-only groups within the first week postsurgery. Evaluation of histological sections showed occasional but mild inflammatory infiltration in lymph nodes, spleen, and liver in all groups. However, no significant histopathological signs were noted beyond the suspected alterations associated with the surgical operation. In particular, no evidence of viral inclusions was observed for any of the evaluated tissues and organs.

#### Hematology and blood chemistry

Blood was analyzed from each animal before surgery and through 35 days postoperation (Fig. 1A). Also, blood from six animals in the no-treatment group was collected for comparison. All parameters for hematology and blood chemistry were consistent among groups and were generally within the normal range. Although there were some minor changes, we found no significant differences in complete blood count (CBC) and clinical chemistry parameters in any treatment group throughout the period of observation (Tables 1 and 2). There were several animals in both the high-dose and low-dose groups that revealed significant changes in amylase; however, the majority of the values were within the normal range. On day 28, animals in the low-dose group demonstrated significant elevation in serum glucose, but those levels returned to the baseline range by day 35.

#### Vector expression by bioluminescence

Whole body image analysis of animals treated with AdLuc/collagen matrix revealed a transduction and distribution profile from adenoviral gene delivery over the course of the experiment. Bioluminescent luciferase expression was detected in the head and neck region for all AdLuc/collagen-treated animals (*n* = 6 per group), with the level of expression higher in animals receiving high-dose AdLuc compared with

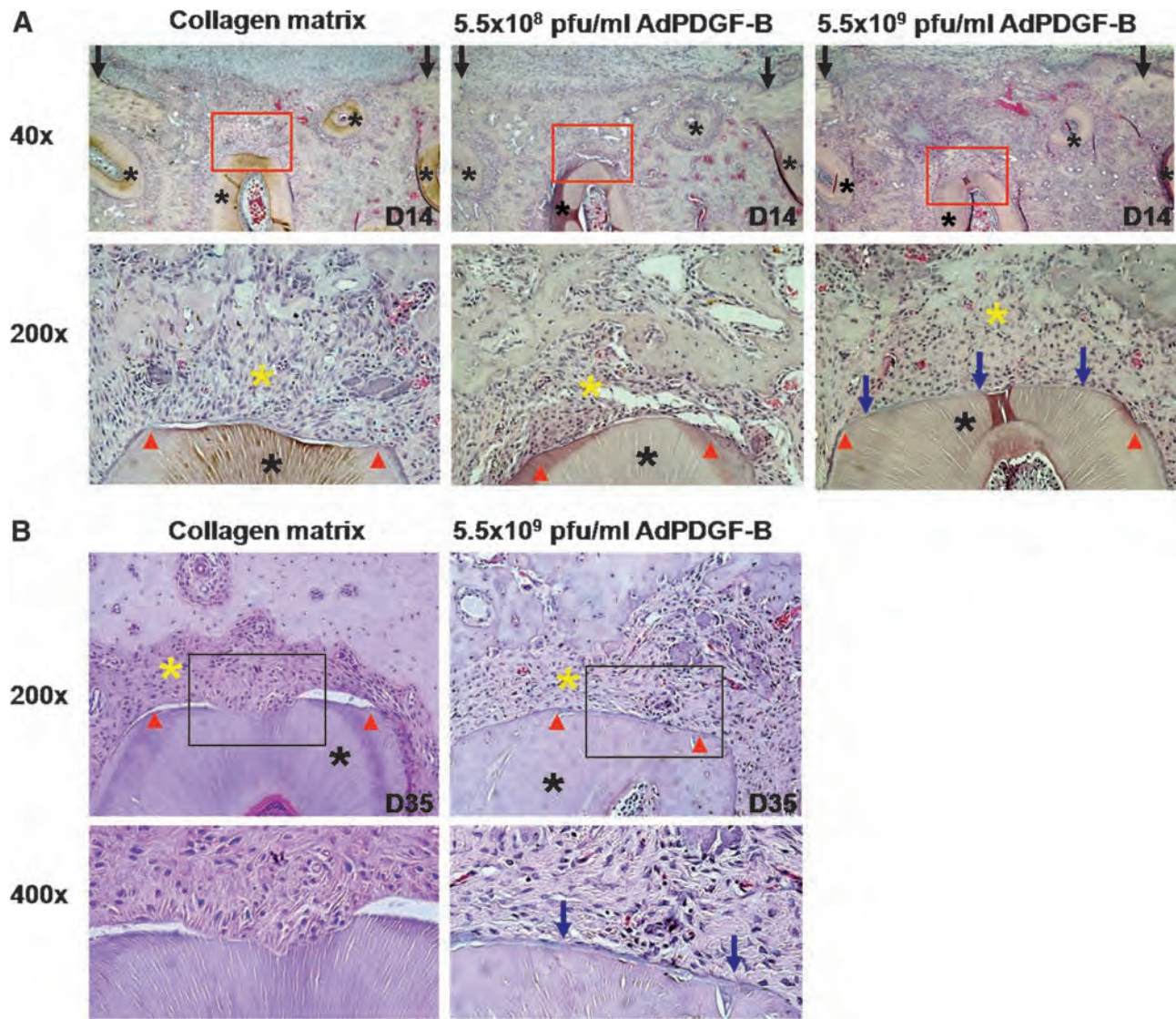


**FIG. 2.** PDGF gene delivery promotes periodontal tissue regeneration *in vivo*. **(A)** Limited bone formation and bridging had occurred by 14 days in wound treated with collagen matrix only compared with AdPDGF-B/collagen-treated defects. *Top:* Original magnification,  $\times 40$ . *Bottom:* Higher power view (original magnification,  $\times 200$ ) of tooth/cementum/periodontal ligament (PDL)/bone interfaces outlined in red in the top row. More newly formed cementum structure (blue arrows) was observed in high-dose ( $5.5 \times 10^9$  PFU/ml) AdPDGF-B/collagen-treated sites. **(B)** At 35 days, defect treated with AdPDGF-B at  $5.5 \times 10^9$  PFU/ml demonstrated a significant amount of root cementum compared with defect treated with collagen matrix only. Red arrowheads indicate the edges of exposed tooth dentin surface; blue arrows, new cementum; black asterisks, tooth roots; yellow asterisks, the area of PDL. (All images are in transverse orientation and stained with hematoxylin and eosin.)

the low-dose animals (Fig. 3A). For the low-dose AdLuc-treated group, luciferase expression gradually decreased to undetectable levels at the treated sites by 14 days without any spreading to distant organs for time points thereafter (note in Fig. 3A whole body imaging [*top*], some luminescence on day 28 on the animal's right side). Results also showed gradually decreasing expression of luciferase in the head and neck region within 2 weeks in high-dose AdLuc-treated animals. Further, the high-dose treated animals yielded a weak signal detected in the axillary lymph node area of three animals, and one animal showed liver expression at 1 week. However, after 2 weeks no signal was detected in any distant organs of any animal (Fig. 3B). To further investigate the persistent, low-level

expression of AdLuc signal in two high-dose treated animals, bioluminescence imaging was performed until sacrifice at 75 days posttreatment. The defect mandible, surrounding musculature, axillary lymph nodes, liver, and gonadal organs were harvested and images were captured for bioluminescence quantification. Results revealed that a weak signal was restricted to only the surrounding musculature ( $< 10$  p/sec/ $\text{mm}^2/\text{sr}$ ), and no signal was detected in the defect site (data not shown). In addition, no significant gender differences in AdLuc expression were revealed; however, a somewhat lower signal was noted on day 1 in the head and neck region of female rats receiving high-dose AdLuc treatment ( $p < 0.05$ ; data not shown).

TABLE 1. HEMATOLOGICAL ANALYSES FOR AdPDGF-B DELIVERY TO ALVEOLAR BONE DEFECTS<sup>a</sup>

Hematological parameter <sup>b</sup>	Before surgery			Day 3			Day 7			Day 14		
	Col	L-Ad	H-Ad	Col	L-Ad	H-Ad	Col	L-Ad	H-Ad	Col	L-Ad	H-Ad
	WBC (K/ $\mu$ l)	12.53 (1.84)	12.87 (2.21)	13.99 (2.98)	13.08 (1.98)	8.491 (1.428)	16.27 (2.29)	12.57 (4.75)	12.07 (3.97)	16.90 (2.19)	16.07 (3.15)	13.01 (2.79)
Neutrophil (K/ $\mu$ l)	3.081 (0.887)	4.184 (0.910)	4.534 (1.343)	3.493 (0.665)	2.448 (0.559)	4.985 (0.660)	4.365 (2.170)	2.781 (1.032)	6.019 (0.678)	6.599 (2.293)	4.134 (1.228)	4.811 (0.663)
Lymphocyte (K/ $\mu$ l)	8.641 (1.481)	7.908 (1.593)	8.753 (1.595)	8.784 (1.449)	5.484 (0.949)	10.16 (1.259)	7.455 (2.674)	8.491 (2.754)	9.651 (1.673)	8.683 (1.870)	8.025 (1.575)	8.974 (0.500)
Monocyte (K/ $\mu$ l)	0.765 (0.239)	0.745 (0.166)	0.604 (0.180)	0.735 (0.220)	0.516 (0.175)	0.841 (0.169)	0.558 (0.299)	0.764 (0.312)	1.141 (0.182)	0.687 (0.079)	0.694 (0.174)	0.711 (0.112)
Eosinophil (K/ $\mu$ l)	0.033 (0.023)	0.021 (0.015)	0.074 (0.048)	0.056 (0.048)	0.043 (0.029)	0.134 (0.075)	0.158 (0.119)	0.029 (0.016)	0.05 (0.043)	0.073 (0.079)	0.133 (0.063)	0.083 (0.096)
Basophil (K/ $\mu$ l)	0.005 (0.008)	0.009 (0.010)	0.024 (0.035)	0.008 (0.010)	0.003 (0.005)	0.026 (0.036)	0.043 (0.041)	0.009 (0.008)	0.03 (0.044)	0.027 (0.048)	0.026 (0.031)	0.016 (0.038)
RBC (M/ $\mu$ l)	7.273 (0.599)	8.164 (0.488)	6.88 (0.646)	7.745 (1.210)	6.709 (0.506)	6.223 (0.426)	5.716 (1.068)	7.606 (1.213)	7.344 (0.600)	6.763 (0.481)	7.043 (0.344)	7.344 (0.224)
Hb (g/dl)	14.91 (0.78)	17.35 (1.72)	13.94 (1.42)	15.25 (2.56)	13.29 (1.10)	12.58 (0.97)	11.35 (2.29)	15.38 (1.95)	15.58 (1.09)	13.51 (0.69)	14.45 (0.60)	15.038 (0.532)
Hct (%)	44.91 (4.53)	51.24 (2.98)	41.76 (4.09)	47.2 (7.67)	40.43 (2.88)	37.64 (2.31)	33.5 (6.37)	44.66 (6.58)	44.74 (5.69)	40.54 (3.40)	41.75 (1.46)	43.89 (1.18)
MCV (fl)	61.7 (1.86)	62.79 (1.20)	60.67 (1.37)	60.9 (1.53)	60.31 (1.74)	60.54 (0.73)	58.52 (1.14)	58.85 (1.37)	62.85 (1.13)	59.89 (1.80)	59.36 (1.20)	59.79 (1.18)
MCH (pg)	20.55 (0.99)	21.24 (1.04)	20.27 (0.76)	19.69 (0.81)	19.8 (0.37)	20.19 (0.30)	19.77 (0.58)	20.33 (1.27)	21.23 (0.47)	20.01 (0.98)	20.54 (1.09)	20.48 (0.34)
MCHC (g/dl)	33.33 (1.75)	33.81 (1.81)	33.39 (0.84)	32.28 (0.75)	32.86 (1.06)	33.4 (0.71)	33.82 (1.09)	34.55 (1.61)	34.03 (1.03)	33.47 (1.59)	34.65 (1.56)	34.288 (0.954)
RDW (%)	15.44 (0.55)	16.2 (0.52)	15.01 (0.32)	16.01 (0.63)	15.76 (0.61)	15.88 (0.46)	15.92 (0.50)	17.65 (0.76)	16.89 (0.67)	16.39 (0.98)	16.29 (0.42)	16.63 (0.37)

Abbreviations: Col. collagen matrix-only group; H-Ad, high-dose ( $5.5 \times 10^9$  PFU/ml) AdPDGF-B-treated group; Hb, hemoglobin; Hct, hematocrit; L-Ad, low-dose ( $5.5 \times 10^8$  PFU/ml) AdPDGF-B-treated group; MCH, mean corpuscular hemoglobin; MCHC, mean corpuscular hemoglobin concentration; MCV, mean corpuscular volume; RBC, red blood cells; RDW, red blood cell distribution width; WBC, white blood cells.

<sup>a</sup>n = 6 per group. Entries demonstrate the average value of parameters for each group; numbers in parentheses indicate standard deviations. No significant differences were noted among the AdPDGF-B and collagen matrix groups during early time points, as well as beyond 14 days (data not shown).

<sup>b</sup>K/ $\mu$ l, thousands per microliter (entry  $\times 10^3$ ); M/ $\mu$ l, millions per microliter (entry  $\times 10^6$ ).

TABLE 2. CLINICAL CHEMISTRY ANALYSES FOR Ad-PDGF-B DELIVERY<sup>a</sup>

Clinical chemistry parameter	Before surgery						Day 7						Day 14					
	L-Ad		H-Ad		Col		L-Ad		H-Ad		Col		L-Ad		H-Ad		Col	
	Col	L-Ad	H-Ad	Col	L-Ad	H-Ad	Col	L-Ad	H-Ad	Col	L-Ad	H-Ad	Col	L-Ad	H-Ad	Col	L-Ad	H-Ad
Albumin (g/dl)	2.814 (0.135)	2.763 (0.130)	2.657 (0.181)	2.65 (0.648)	2.657 (0.172)	2.825 (0.116)	2.543 (0.113)	2.95 (0.141)	2.788 (0.181)	2.786 (0.177)	2.913 (0.125)	3.133 (0.234)	2.786 (0.177)	2.913 (0.125)	3.133 (0.234)	2.786 (0.177)	2.913 (0.125)	3.133 (0.234)
ALPase (U/liter)	260.43 (23.52)	255 (53.18)	239 (31.09)	185.5 (59.34)	238.43 (35.45)	166.63 (29.61)	200.86 (37.66)	205.75 (58.94)	153.38 (27.69)	232.29 (29.19)	232.63 (42.45)	251.67 (43.48)	232.29 (29.19)	232.63 (42.45)	251.67 (43.48)	232.29 (29.19)	232.63 (42.45)	251.67 (43.48)
ALT (U/liter)	67.14 (8.30)	89 (8.45)	87.25 (7.50)	72.88 (8.92)	79.86 (4.06)	79.88 (8.15)	100.57 (10.47)	79.38 (9.96)	81 (5.04)	84.86 (5.05)	86.5 (7.58)	79.5 (19.99)	84.86 (5.05)	86.5 (7.58)	79.5 (19.99)	84.86 (5.05)	86.5 (7.58)	79.5 (19.99)
Amylase (U/liter)	1881.14 (186.95)	1831 (188.36)	1554.17 (267.61)	1905.38 (388.61)	1857.43 (544.49)	1770 (251.95)	2494.86 <sup>b</sup> (844.40)	1705.75 (310.88)	1785.13 (328.22)	1990.71 (525.58)	1879.38 (195.60)	2085.33 (44.004)	1990.71 (525.58)	1879.38 (195.60)	2085.33 (44.004)	1990.71 (525.58)	1879.38 (195.60)	2085.33 (44.004)
AST (U/liter)	71.86 (9.91)	79.38 (9.32)	79.88 (8.97)	69.5 (20.76)	83.5 (16.55)	69.88 (5.19)	126.14 (11.67)	77.57 (13.23)	70.5 (11.43)	66.43 (11.77)	90.5 (26.46)	93.25 (16.34)	66.43 (11.77)	90.5 (26.46)	93.25 (16.34)	66.43 (11.77)	90.5 (26.46)	93.25 (16.34)
Bilirubin (mg/dl)	20.14 (3.34)	19.5 (3.70)	19 (2.16)	21.25 (2.49)	20 (2)	22.13 (2.59)	24.86 (1.86)	21.38 (2.39)	19.13 (1.64)	22.57 (1.62)	23.75 (3.45)	24.17 (1.33)	22.57 (1.62)	23.75 (3.45)	24.17 (1.33)	22.57 (1.62)	23.75 (3.45)	24.17 (1.33)
Calcium (mg/dl)	10.11 (0.25)	10.29 (0.19)	10.16 (0.28)	10.54 (1.30)	10.23 (0.28)	10.49 (0.15)	10.41 (0.25)	10.35 (0.23)	10.35 (0.12)	10.86 (0.24)	10.28 (0.18)	10.83 (0.23)	10.86 (0.24)	10.28 (0.18)	10.83 (0.23)	10.86 (0.24)	10.28 (0.18)	10.83 (0.23)
Cholesterol (mg/dl)	83.29 (7.13)	78 (9.20)	63.86 (11.81)	78.71 (29.37)	80.29 (8.16)	90 (7.01)	80 (6.90)	80.38 (7.03)	81.13 (2.80)	84.43 (10.88)	77.38 (10.32)	82.33 (5.86)	84.43 (10.88)	77.38 (10.32)	82.33 (5.86)	84.43 (10.88)	77.38 (10.32)	82.33 (5.86)
Creatine kinase (U/liter)	166.67 (28.25)	190.63 (51.90)	176.86 (47.36)	178.5 (70.13)	259.83 (133.13)	142.63 (33.18)	156.20 (38.46)	244.57 (106.69)	219.38 (64.16)	121.71 (28.96)	186.88 (61.42)	197.75 (61.41)	121.71 (28.96)	186.88 (61.42)	197.75 (61.41)	121.71 (28.96)	186.88 (61.42)	197.75 (61.41)
Creatinine (mg/dl)	0.4 (0.058)	0.35 (0.053)	0.329 (0.049)	0.363 (0.052)	0.386 (0.038)	0.4 (0)	0.386 (0.038)	0.388 (0.035)	0.3 (0.053)	0.4 (0)	0.388 (0.035)	0.629 (0.399)	0.388 (0.035)	0.388 (0.035)	0.629 (0.399)	0.388 (0.035)	0.388 (0.035)	0.629 (0.399)
Glucose (mg/dl)	230.43 (18.39)	227.88 (27.22)	229 (35.77)	217.65 (24.22)	221.57 (19.15)	191 (33.815)	245.29 (53.94)	232 (29.99)	229.88 (30.19)	192.14 (7.67)	212.5 (39.75)	200.4 (10.69)	192.14 (7.67)	212.5 (39.75)	200.4 (10.69)	192.14 (7.67)	212.5 (39.75)	200.4 (10.69)
Phosphorus (mg/dl)	7.657 (0.660)	7.4 (0.490)	6.743 (0.395)	7.225 (0.585)	6.214 (0.157)	6.663 (0.434)	6.671 (0.340)	7.65 (0.537)	7.45 (0.407)	5.9 (2.62)	7.325 (0.486)	6.833 (0.115)	5.9 (2.62)	7.325 (0.486)	6.833 (0.115)	5.9 (2.62)	7.325 (0.486)	6.833 (0.115)
T. bilirubin (mg/dl)	0.1 (0)	0.1 (0)	0.1 (0)	0.275 (0.456)	0.114 (0.038)	0.113 (0.035)	0.1 (0)	0.175 (0.139)	0.213 (0.210)	0.1 (0)	0.113 (0.035)	0.1 (0)	0.175 (0.139)	0.213 (0.210)	0.1 (0)	0.175 (0.139)	0.213 (0.210)	0.1 (0)
Total protein (g/dl)	5.629 (0.325)	5.625 (0.205)	5.557 (0.276)	5.95 (0.680)	5.529 (0.250)	5.925 (0.128)	5.586 (0.219)	5.863 (0.250)	5.8 (0.278)	5.943 (0.190)	5.938 (0.262)	6.443 (0.351)	5.943 (0.190)	5.938 (0.262)	6.443 (0.351)	5.943 (0.190)	5.938 (0.262)	6.443 (0.351)
Globulin (g/dl)	2.814 (0.227)	2.838 (0.106)	2.886 (0.107)	3.288 (1.272)	2.957 (0.162)	3.1 (0.093)	3.043 (0.151)	2.925 (0.128)	3.025 (0.128)	3.157 (0.140)	3.013 (0.146)	3.25 (0.152)	3.157 (0.140)	3.013 (0.146)	3.25 (0.152)	3.157 (0.140)	3.013 (0.146)	3.25 (0.152)

*Abbreviations:* ALPase, alkaline phosphatase; ALT, alanine transaminase; AST, aspartate transaminase; Col, collagen matrix-only group; H-Ad, high-dose ( $5.5 \times 10^8$  PFU/ml) AdPDGF-B-treated group; L-Ad, low-dose ( $5.5 \times 10^6$  PFU/ml) AdPDGF-B-treated group; T. bilirubin, total bilirubin.

<sup>a</sup>All comparisons are made with reference to the collagen matrix group. Entries demonstrate the mean value of parameters for each group; numbers in parentheses indicates standard deviations. Serum amylase for both AdPDGF-B-treated groups revealed significant differences with respect to the collagen matrix group, and was within the normal range for time points beyond 14 days.

<sup>b</sup>Significant difference from collagen matrix group ( $p < 0.05$ ;  $n = 6$  per group).

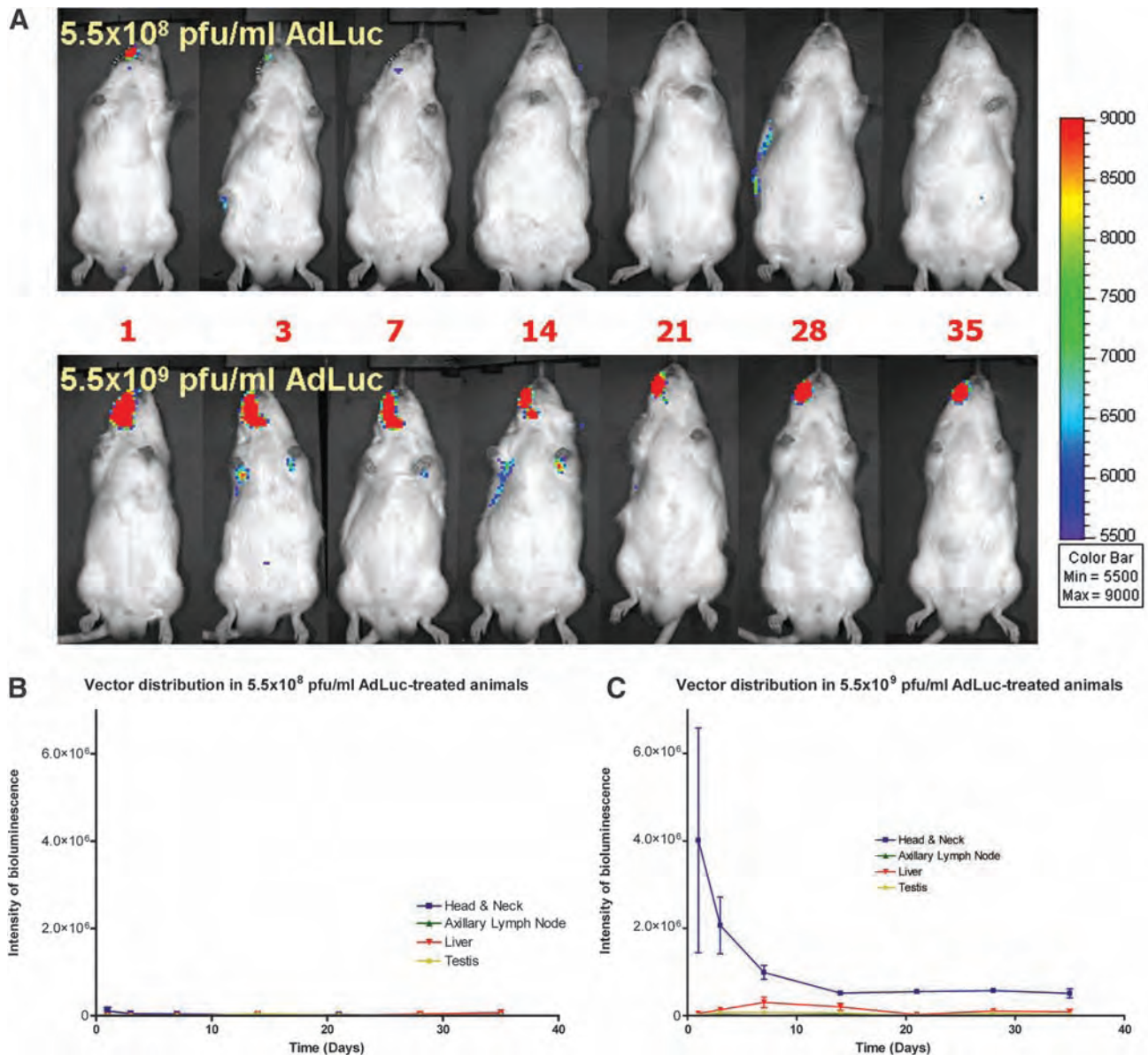


**FIG. 3.** Vector transduction efficiency and systemic distribution of bioluminescence. **(A)** Most of the luciferin signal is restricted to the alveolar bone defect region, with minimal systemic involvement. Signals in distant organs were absent after 14 days for both dose level groups. **(B)** Mild vector expression was noted during the first 3–7 days in animals treated with AdLuc at  $5.5 \times 10^8$  PFU/ml. **(C)** Animals treated with AdLuc at  $5.5 \times 10^9$  PFU/ml demonstrated significant vector expression during the first 14 days, followed by a decrease in vector expression in the head and neck region over time. The high-dose group also showed modest vector expression in liver (one of six positive on day 14) and axillary lymph nodes (one of six positive on day 3, and two of six positive on both days 7 and 10). Group size:  $n = 6$  (three per gender). If the intensity of bioluminescence within the region of interest was less than 5000 p/sec/cm<sup>2</sup>/sr, that region was defined as “negative”.

#### Biodistribution by quantitative PCR

The specificity of our PCR primers and the sensitivity of the assay were determined before analysis of the study samples. We measured no primer cross-reaction with adenovirus encoding bone sialoprotein, bone morphogenetic protein-7, luciferase, noggin, PDGF-A, PDGF-1308, or GFP (data not shown). The sensitivity and detection limit of our PCR assays was 30 virus copies per 500 ng of DNA. Within the AdPDGF-B-treated area, viral vector could be detected within the first

week in DNA from both high-dose and low-dose treated animals. The number of vector copies gradually decreased to undetectable levels after 2 weeks (Table 3). Vector copies measured in the blood were below the detection limit for all animals over the total period of observation. The PCR assay measured a low level of vector within spleen DNA of one animal at 3 days posttreatment, and within the lung of another animal at 2 weeks posttreatment; however, no significant vector DNA was detected in organs or tissues from the treatment groups for the remainder of the experimental time points

TABLE 3. AdPDGF-B PCR RESULTS IN BLOODSTREAM AND DISTANT ORGANS

Organ/tissue	Treatment	No treatment	Day 3	Day 7	Day 14	Day 21	Day 28	Day 35
Whole tissue from osseous defect	Collagen matrix	N	N	N	N	N	N	N
	$5.5 \times 10^8$ PFU/ml AdPDGF-B	N	3/3 (301)	2/3 (137)	1/3 (84)	N	N	N
	$5.5 \times 10^9$ PFU/ml AdPDGF-B	N	3/3 (45,930)	3/3 (6,097)	N	N	N	N
Blood	Collagen matrix	N	N	N	N	N	N	N
	$5.5 \times 10^8$ PFU/ml AdPDGF-B	N	N	N	N	N	N	N
	$5.5 \times 10^9$ PFU/ml AdPDGF-B	N	N	N	N	N	N	N
Lung	Collagen matrix	N	N	N	N	N	N	N
	$5.5 \times 10^8$ PFU/ml AdPDGF-B	N	N	N	1/3 (38)	N	N	N
	$5.5 \times 10^9$ PFU/ml AdPDGF-B	N	N	N	N	N	N	N
Spleen	Collagen matrix	N	N	N	N	N	N	N
	$5.5 \times 10^8$ PFU/ml AdPDGF-B	N	1/3 (31)	N	N	N	N	N
	$5.5 \times 10^9$ PFU/ml AdPDGF-B	N	N	N	N	N	N	N
Brain, SLN, ALN, heart, liver, kidney, sex organs (testes or ovaries)	Collagen matrix	N	N	N	N	N	N	N
	$5.5 \times 10^8$ PFU/ml AdPDGF-B	N	N	N	N	N	N	N
	$5.5 \times 10^9$ PFU/ml AdPDGF-B	N	N	N	N	N	N	N

Abbreviations: ALN, axillary lymph nodes; N, negative; PFU, plaque-forming units; SLN, submandibular lymph nodes.

<sup>a</sup>*n* = 3 per group (for organ analyses) and 23 per group (for blood analyses). Test sample DNAs yielding signals below the limit of detection (<30 vector particles per 500 ng of DNA) are reported as negative. Entries demonstrate "positive" animals in each group and entries in parentheses indicate the mean vector copy number per 500 ng of DNA from the positive animals.

(Table 3). These values were below the detection limit and compared similarly with vector values at the defect site, which were low to below the detection level. On examination of histological sections from the tissues (spleen and lung) positive for AdPDGF-B DNA, we found no inflammation-related phenotype or other pathological findings when compared with tissue sections from collagen matrix-treated animals.

## Discussion

PDGF-BB protein has demonstrated its strong potential for soft and hard tissue repair and is available for clinical use (Nevins *et al.*, 2005; Hollinger *et al.*, 2008). However, because of the high degradation rate and transient persistence *in vivo*, the treatment outcome is not entirely predictable for clinical applications (Kaigler *et al.*, 2006). Gene delivery using an adenoviral vector provides sustained and stable transduction efficiency *in vitro* (Chen and Giannobile, 2002). These data confirm and extend those of Jin and colleagues (2004) demonstrating significant enhancement of tooth-supporting alveolar bone and cementum regeneration *in vivo*, using gene-activated matrices containing AdPDGF-B.

Although a number of studies focus on the safety profile of adenovirus-mediated gene therapy, few of them have addressed the local delivery of vectors using a gene-activated matrix and none are related to the periodontium or localized bone defects. Studies have shown that direct systemic administration of adenoviral vectors can result in acute toxicity and hepatic pathology (Nunes *et al.*, 1999; Lenaerts *et al.*, 2005; Ni *et al.*, 2005). Systemic dissemination can be reduced and the efficacy-to-toxicity ratio can be improved by local gene delivery (Wang *et al.*, 2005). With localized delivery, the vector likely enters the systemic circulation via the leaky microvessels and systemically disseminates within 10 min (Wang *et al.*, 2005), with the inflammatory infiltrate within liver observed after 15 min in mice (Ni *et al.*, 2005). In this study,

we employed matrix (collagen)-enabled gene delivery for localized administration to alveolar bone defects. The vector dissemination in our animals beyond the alveolar bone area was limited, demonstrating well-contained localization of the gene-activated matrix.

Studies have shown that nearly 99% of systemically delivered adenoviral vectors will eventually accumulate in the liver, and are rapidly taken up by Kupffer cells and hepatocytes (Hackett *et al.*, 2000; Manickan *et al.*, 2006). The Kupffer cells might distribute to the lung and spleen via the circulation, but in this study we did not detect any significant vector quantities in those organs. No significant elevation of the enzymes specific to those organs further demonstrates the limited systemic influence of this approach. Although transgene luciferase expression was found in the axillary lymph nodes, spleen, and lungs of a few adenoviral vector-treated animals at 2 weeks postadministration (with no expression in these organs at later time points), the level was only slightly greater than background and no accompanying toxicological signs or histopathological changes were found. We also noted no treatment-related toxicity throughout the 35-day period. Most of the hematological and clinical chemistry parameters were within normal ranges and the only significant difference was noted for amylase (derived primarily from the pancreas and parotid gland, with some from the liver), which is one of the major enzymes to digest starch into simple sugars. Changes in serum amylase may represent a normal physiologic process, acute or chronic pancreatitis, or concomitant ongoing diseases (Garrison, 1986). However, lipase is a more sensitive and specific marker with which to diagnose pancreatitis (Tietz *et al.*, 1986), and the lipase level in all of the animals did not change significantly. However, it is quite possible that the amylase came from the parotid salivary gland that was located in close proximity to the surgical field. The parotid gland in rats is nonencapsulated, as compared with the gland in humans. We cannot rule out this area at

early time points. At later time points when we measured the luciferase signal from the harvested organs, no detectable signal was found in any of the parotid glands, but mainly in the surrounding musculature (Fig. 3). *In vivo* bioluminescence generated by expression of the luciferase transgene permitted quantification and localization of transgene expression and provided noninvasive, dynamic, and comprehensive monitoring of vector expression at the whole body level (Wood *et al.*, 1999; Johnson *et al.*, 2006). As little as  $10^4$  luciferase-expressing recombinant adenoviruses are capable of producing luminescence in the liver (Honigman *et al.*, 2001), which is significantly higher in sensitivity than is possible with qPCR (Johnson *et al.*, 2006), making bioluminescence a more sensitive mode of evaluation of biodistribution and subsequent vector activity. In the early time periods we detected vector in the defect area of adenovirus-treated animals, which reached undetectable levels by day 14. This result supports those reported by Jin and colleagues (2004), showing that the luciferase signal decreased to 20% by day 14 and reached an undetectable level by day 28 compared with the expression on day 1. Moreover, given that PDGF is expressed *in vivo* over about 10 days in periodontal wounds after injury (Green *et al.*, 1997), this gene therapy approach demonstrates a similar expression profile that may be favorable for therapeutic application.

In summary, the results of our experiments demonstrate that local administration of AdPDGF-B with gene-activated matrix is safe when delivered to tooth-supporting alveolar bone defects. No treatment-related toxicity or systemic involvement was found. Although vector particle DNA was detectable during the first 2 weeks, primarily in the osseous defects, the titer was low and quickly attenuated at subsequent time points. These results support the further clinical development of AdPDGF-B for regeneration therapy for oral and craniofacial bone application.

### Acknowledgments

The authors thank Anna Colvig for performing hematological and clinical chemical examinations, Amanda Welton for assistance with bioluminescence, Dr. John E. Wilkinson for assistance with veterinary pathology, and Christopher Strayhorn for assistance with histological processing. This study was supported in part by grants from the AO Foundation (Davos, Switzerland) and NIH/NIDCR R01-DE13397.

### Author Disclosure Statement

Drs. Sosnowski and Chandler are employees of Tissue Repair Co. The University of Michigan will benefit financially by clinical development of this technology.

### References

Andrae, J., Gallini, R., and Betsholtz, C. (2008). Role of platelet-derived growth factors in physiology and medicine. *Genes Dev.* 22, 1276–1312.

Chandler, L.A., Doukas, J., Gonzalez, A.M., Hoganson, D.K., Gu, D.L., Ma, C., Nesbit, M., Crombleholme, T.M., Herlyn, M., Sosnowski, B.A., and Pierce, G.F. (2000). FGF2-targeted adenovirus encoding platelet-derived growth factor-B enhances *de novo* tissue formation. *Mol. Ther.* 2, 153–160.

Chen, Q.P., and Giannobile, W.V. (2002). Adenoviral gene transfer of PDGF downregulates gas gene product PDGF $\alpha$ R and prolongs ERK and Akt/PKB activation. *Am. J. Physiol. Cell Physiol.* 282, C538–C544.

Cooke, J.W., Sarment, D.P., Whitesman, L.A., Miller, S.E., Jin, Q., Lynch, S.E., and Giannobile, W.V. (2006). Effect of rhPDGF-BB delivery on mediators of periodontal wound repair. *Tissue Eng.* 12, 1441–1450.

Cotrim, A.P., and Baum, B.J. (2008). Gene therapy: Some history, applications, problems, and prospects. *Toxicol. Pathol.* 36, 97–103.

Cotrim, A.P., Sowers, A., Mitchell, J.B., and Baum, B.J. (2007). Prevention of irradiation-induced salivary hypofunction by microvessel protection in mouse salivary glands. *Mol. Ther.* 15, 2101–2106.

Fiedler, J., Etzel, N., and Brenner, R.E. (2004). To go or not to go: Migration of human mesenchymal progenitor cells stimulated by isoforms of PDGF. *J. Cell Biochem.* 93, 990–998.

Garrison, R. (1986). Amylase. *Emerg. Med. Clin. North Am.* 4, 315–327.

Giannobile, W.V., Finkelman, R.D., and Lynch, S.E. (1994). Comparison of canine and nonhuman primate models for periodontal regenerative therapy: results following a single administration of PDGF/IGF-I. *J. Periodontol.* 65, 1158–1168.

Giannobile, W.V., Hernandez, R.A., Finkelman, R.D., Ryan, S., Kiritsy, C.P., D'Andrea, M.D., and Lynch, S.E. (1996). Comparative Effects of PDGF-BB, IGF-I singularly and in combination on periodontal regeneration in *Macaca fascicularis*. *J. Periodont. Res.* 31, 301–312.

Green, R.J., Usui, M.L., Hart, C.E., Ammons, W.F., and Narayanan, A.S. (1997). Immunolocalization of platelet-derived growth factor A and B chains and PDGF- $\alpha$  and  $\beta$  receptors in human gingival wounds. *J. Periodont. Res.* 32, 209–214.

Gu, D.L., Nguyen, T., Gonzalez, A.M., Printz, M.A., Pierce, G.F., Sosnowski, B.A., Phillips, M.L., and Chandler, L.A. (2004). Adenovirus encoding human platelet-derived growth factor-B delivered in collagen exhibits safety, biodistribution, and immunogenicity profiles favorable for clinical use. *Mol. Ther.* 9, 699–711.

Haase, H.R., Clarkson, R.W., Waters, M.J., and Bartold, P.M. (1998). Growth factor modulation of mitogenic responses and proteoglycan synthesis by human periodontal fibroblasts. *J. Cell Physiol.* 174, 353–361.

Hackett, N.R., El Sawy, T., Lee, L.Y., Silva, I., O'Leary, J., Rosengart, T.K., and Crystal, R.G. (2000). Use of quantitative TaqMan real-time PCR to track the time-dependent distribution of gene transfer vectors *in vivo*. *Mol. Ther.* 2, 649–656.

Hollinger, J.O., Hart, C.E., Hirsch, S.N., Lynch, S., and Friedlaender, G.E. (2008). Recombinant human platelet-derived growth factor: Biology and clinical applications. *J. Bone Joint Surg. Am.* 90(Suppl. 1):48–54.

Honigman, A., Zeira, E., Ohana, P., Abramovitz, R., Tavor, E., Bar, I., Zilberman, Y., Rabinovsky, R., Gazit, D., Joseph, A., Panet, A., Shai, E., Palmon, A., Laster, M., and Galun, E. (2001). Imaging transgene expression in live animals. *Mol. Ther.* 4, 239–249.

Howell, T.H., Fiorellini, J.P., Paquette, D.W., Offenbacher, S., Giannobile, W.V., and Lynch, S.E. (1997). A phase I/II clinical trial to evaluate a combination of recombinant human platelet-derived growth factor-BB and recombinant human insulin-like growth factor-I in patients with periodontal disease. *J. Periodontol.* 68, 1186–1193.

Jin, Q., Anusaksathien, O., Webb, S.A., Rutherford, R.B., and Giannobile, W.V. (2003). Gene therapy of bone morphogenetic protein for periodontal tissue engineering. *J. Periodontol.* 74, 202–213.

- Jin, Q., Anusaksathien, O., Webb, S.A., Printz, M.A., and Giannobile, W.V. (2004). Engineering of tooth-supporting structures by delivery of PDGF gene therapy vectors. *Mol. Ther.* 9, 519–526.
- Johnson, M., Huyn, S., Burton, J., Sato, M., and Wu, L. (2006). Differential biodistribution of adenoviral vector *in vivo* as monitored by bioluminescence imaging and quantitative polymerase chain reaction. *Hum. Gene Ther.* 17, 1262–1269.
- Kaigler, D., Cirelli, J.A., and Giannobile, W.V. (2006). Growth factor delivery for oral and periodontal tissue engineering. *Exp. Opin. Drug Deliv.* 3, 647–662.
- Lenaerts, L., Verbeken, E., De Clercq, E., and Naesens, L. (2005). Mouse adenovirus type 1 infection in SCID mice: An experimental model for antiviral therapy of systemic adenovirus infections. *Antimicrob. Agents Chemother.* 49, 4689–4699.
- Manickan, E., Smith, J.S., Tian, J., Eggerman, T.L., Lozier, J.N., Muller, J., and Byrnes, A.P. (2006). Rapid Kupffer cell death after intravenous injection of adenovirus vectors. *Mol. Ther.* 13, 108–117.
- Nevins, M., Giannobile, W.V., McGuire, M.K., Kao, R.T., Mellonig, J.T., Hinrichs, J.E., McAllister, B.S., Murphy, K.S., McClain, P.K., Nevins, M.L., Paquette, D.W., Han, T.J., Reddy, M.S., Lavin, P.T., Genco, R.J., and Lynch, S.E. (2005). Platelet-derived growth factor stimulates bone fill and rate of attachment level gain: Results of a large multicenter randomized controlled trial. *J. Periodontol.* 76, 2205–2215.
- Ni, S., Bernt, K., Gagar, A., Li, Z.Y., Kiem, H.P., and Lieber, A. (2005). Evaluation of biodistribution and safety of adenovirus vectors containing group B fibers after intravenous injection into baboons. *Hum. Gene Ther.* 16, 664–677.
- Nishimura, F., and Terranova, V.P. (1996). Comparative study of the chemotactic responses of periodontal ligament cells and gingival fibroblasts to polypeptide growth factors. *J. Dent. Res.* 75, 986–992.
- Nunes, F.A., Furth, E.E., Wilson, J.M., and Raper, S.E. (1999). Gene transfer into the liver of nonhuman primates with E1-deleted recombinant adenoviral vectors: Safety of re-administration. *Hum. Gene Ther.* 10, 2515–2526.
- Park, Y.J., Lee, Y.M., Park, S.N., Sheen, S.Y., Chung, C.P., and Lee, S.J. (2000). Platelet derived growth factor releasing chitosan sponge for periodontal bone regeneration. *Biomaterials* 21, 153–159.
- Ramseier, C.A., Abramson, Z.R., Jin, Q., and Giannobile, W.V. (2006). Gene therapeutics for periodontal regenerative medicine. *Dent. Clin. North Am.* 50, 245–263, ix.
- Ronnstrand, L., and Heldin, C.H. (2001). Mechanisms of platelet-derived growth factor-induced chemotaxis. *Int. J. Cancer* 91, 757–762.
- Southwood, L.L., Frisbie, D.D., Kawcak, C.E., and McIlwraith, C.W. (2004). Delivery of growth factors using gene therapy to enhance bone healing. *Vet. Surg.* 33, 565–578.
- Tietz, N.W., Huang, W.Y., Rauh, D.F., and Shuey, D.F. (1986). Laboratory tests in the differential diagnosis of hyperamylasemia. *Clin. Chem.* 32, 301–307.
- Voutetakis, A., Zheng, C., Metzger, M., Cotrim, A.P., Donahue, R.E., Dunbar, C.E., and Baum, B.J. (2008). Sorting of transgenic secretory proteins in rhesus macaque parotid glands following adenoviral mediated gene transfer. *Hum. Gene Ther.* 19, 1401–1405.
- Wang, Y., Yang, Z., Liu, S., Kon, T., Krol, A., Li, C.Y., and Yuan, F. (2005). Characterisation of systemic dissemination of non-replicating adenoviral vectors from tumours in local gene delivery. *Br. J. Cancer* 92, 1414–1420.
- Wood, M., Perrotte, P., Onishi, E., Harper, M.E., Dinney, C., Pagliaro, L., and Wilson, D.R. (1999). Biodistribution of an adenoviral vector carrying the luciferase reporter gene following intravesical or intravenous administration to a mouse. *Cancer Gene Ther.* 6, 367–372.

Address reprint requests to:  
Dr. William V. Giannobile  
University of Michigan  
1011 N. University Avenue  
Room 3305, Dental Building  
Ann Arbor, MI 48109

E-mail: william.giannobile@umich.edu

Received for publication July 25, 2008;  
accepted after revision January 23, 2009.

Published online: April 1, 2009.

## **RESULTS, DISCUSSIONS, and CONCLUSIONS**

B: PDGF-B gene therapy accelerates bone engineering and oral implant osseointegration. (Chang et al. Gene Ther. 2009 (in press))

Results and Discussion are on pages 28 ~ 34.

ORIGINAL ARTICLE

# PDGF-B gene therapy accelerates bone engineering and oral implant osseointegration

P-C Chang<sup>1,2,8</sup>, Y-J Seol<sup>1,3,8</sup>, JA Cirelli<sup>1,4</sup>, G Pellegrini<sup>1,5</sup>, Q Jin<sup>1</sup>, LM Franco<sup>1</sup>, SA Goldstein<sup>2,6</sup>, LA Chandler<sup>7</sup>, B Sosnowski<sup>7</sup> and WV Giannobile<sup>1,2</sup>

<sup>1</sup>Department of Periodontics and Oral Medicine, School of Dentistry, University of Michigan, Ann Arbor, MI, USA; <sup>2</sup>Department of Biomedical Engineering, College of Engineering, University of Michigan, Ann Arbor, MI, USA; <sup>3</sup>Department of Periodontology, School of Dentistry, Seoul National University, Seoul, Korea; <sup>4</sup>Department of Periodontology, School of Dentistry at Araraquara, State University of São Paulo, Araraquara, São Paulo, Brazil; <sup>5</sup>Department of Periodontology, Clinics Hospital Mangiagalli, University of Milan, Milan, Italy; <sup>6</sup>Department of Orthopaedic Surgery, School of Medicine, University of Michigan, Ann Arbor, MI, USA and <sup>7</sup>Tissue Repair Company, San Diego, CA, USA

Platelet-derived growth factor-BB (PDGF-BB) stimulates repair of healing-impaired chronic wounds such as diabetic ulcers and periodontal lesions. However, limitations in predictability of tissue regeneration occur due, in part, to transient growth factor bioavailability *in vivo*. Here, we report that gene delivery of PDGF-B stimulates repair of oral implant extraction socket defects. Alveolar ridge defects were created in rats and were treated at the time of titanium implant installation with a collagen matrix containing an adenoviral (Ad) vector encoding PDGF-B ( $5.5 \times 10^8$  or  $5.5 \times 10^9$  pfu ml<sup>-1</sup>), Ad encoding luciferase (Ad-Luc;  $5.5 \times 10^9$  pfu ml<sup>-1</sup>; control) or recombinant human PDGF-BB protein (rhPDGF-BB, 0.3 mg ml<sup>-1</sup>). Bone repair and osseointegration were measured through backscattered

scanning electron microscopy, histomorphometry, micro-computed tomography and biomechanical assessments. Furthermore, a panel of local and systemic safety assessments was performed. Results indicated that bone repair was accelerated by Ad-PDGF-B and rhPDGF-BB delivery compared with Ad-Luc, with the high dose of Ad-PDGF-B more effective than the low dose. No significant dissemination of the vector construct or alteration of systemic parameters was noted. In summary, gene delivery of Ad-PDGF-B shows regenerative and safety capabilities for bone tissue engineering and osseointegration in alveolar bone defects comparable with rhPDGF-BB protein delivery *in vivo*. Gene Therapy (2010) 17, 95–104; doi:10.1038/gt.2009.117; published online 10 September 2009

**Keywords:** dental implant; platelet-derived growth factor; regenerative medicine; virus delivery

## Introduction

Oral implants are widely accepted in dental medicine as a reconstructive treatment modality for tooth replacement due to disease, injury or congenital defects. In clinical situations exhibiting limited alveolar bone availability, growth factor application has been advocated to improve osteogenesis and osseointegration.<sup>1</sup> However, as a result of the transient action and the high degradation rate of recombinant proteins *in vivo*,<sup>2</sup> the sustained bioactivity of gene therapy vectors has been purported to be an effective alternative for the delivery of growth factor proteins.<sup>3,4</sup> Adenoviral (Ad) vectors have been shown to exhibit a high *in vivo* transduction efficiency,<sup>5</sup> with a relatively short expression period compared with other viral-based gene delivery methods, and their effectiveness for promoting initial wound healing without eliciting long-term health concerns in wound healing models.<sup>6,7</sup>

Platelet-derived growth factor (PDGF) is a potent mitogen that facilitates wound healing<sup>8</sup> and stimulates

bone repair by expanding osteoblastic precursor cells.<sup>9,10</sup> PDGF-BB is Food and Drug Administration-approved for use in the treatment of localized periodontal defects and diabetic ulcers<sup>11–13</sup> Ad-mediated PDGF-B (Ad-PDGF-B) gene delivery has been shown to enhance periodontal tissue regeneration of tooth-supporting wounds.<sup>6,14</sup>

Limited information is available regarding the potential of PDGF-BB on promoting osseointegration of oral implants. In addition, the influence of PDGF-B on the mechanical integrity of an implant interface is unknown. The purpose of this study was to investigate the effects of rhPDGF-BB and Ad-PDGF-B delivered in a collagen matrix on the osteogenesis and osseointegration of dental implants in an *in vivo* osseointegration model. This approach shows the ability of Ad-PDGF-B to accelerate oral implant osseointegration. The data support the concept that Ad-PDGF-B gene delivery may be an effective and safe mode of therapy comparable with PDGF-BB application to promote dental implant osseointegration and oral bone repair.

## Results

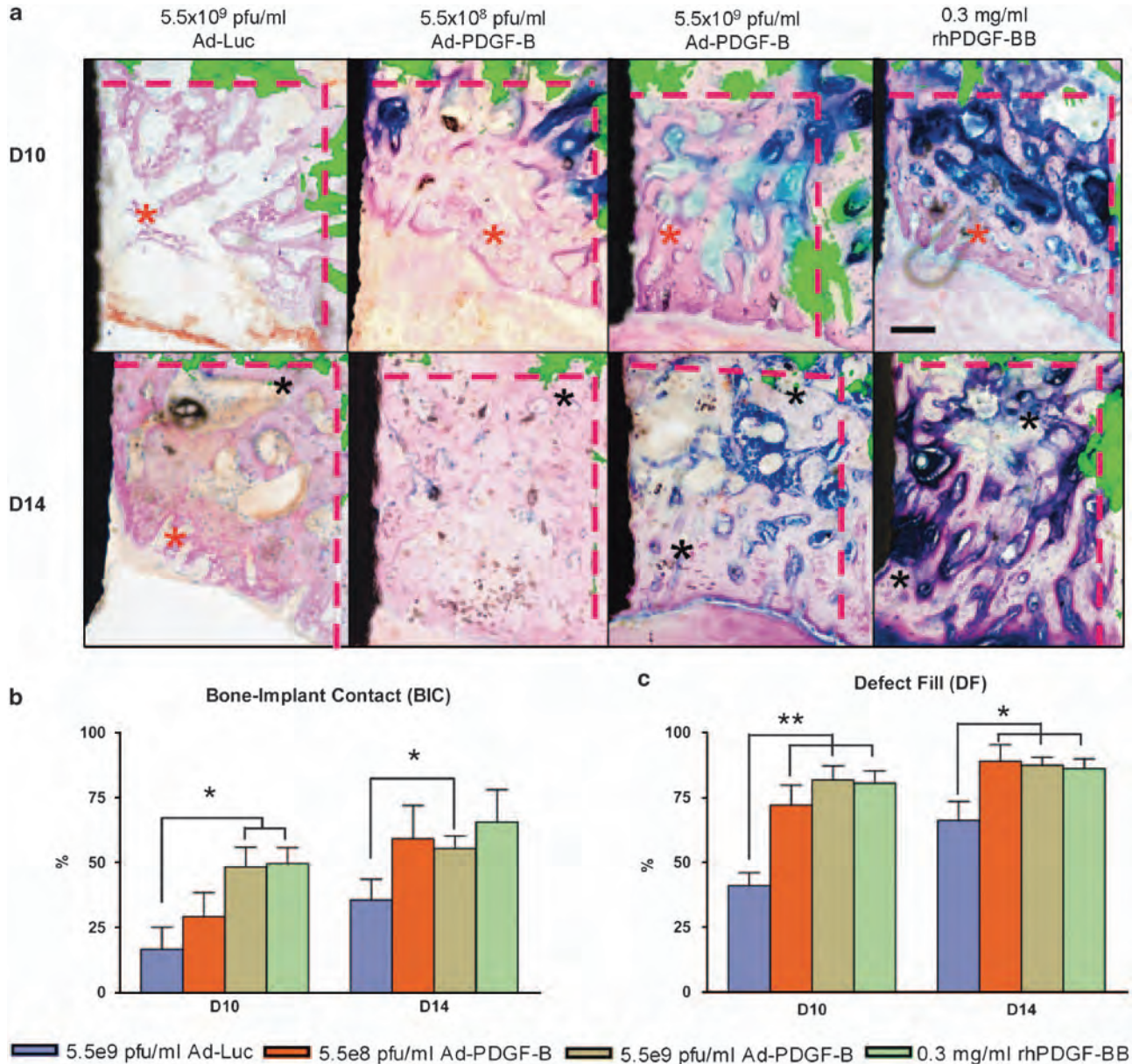
### Ad-PDGF-B and rhPDGF-BB enhance osteogenesis *in vivo*

On the basis of the descriptive histology (Figure 1a), by day 10 a gradual defect resolution was observed over time in all groups. At days 10 and 14, woven bone and

Correspondence: Professor WV Giannobile, Department of Periodontics and Oral Medicine, School of Dentistry, University of Michigan, 1011 N. University Ave., Ann Arbor, MI 48109, USA.  
E-mail: william.giannobile@umich.edu

<sup>8</sup>These authors contributed equally to this work.

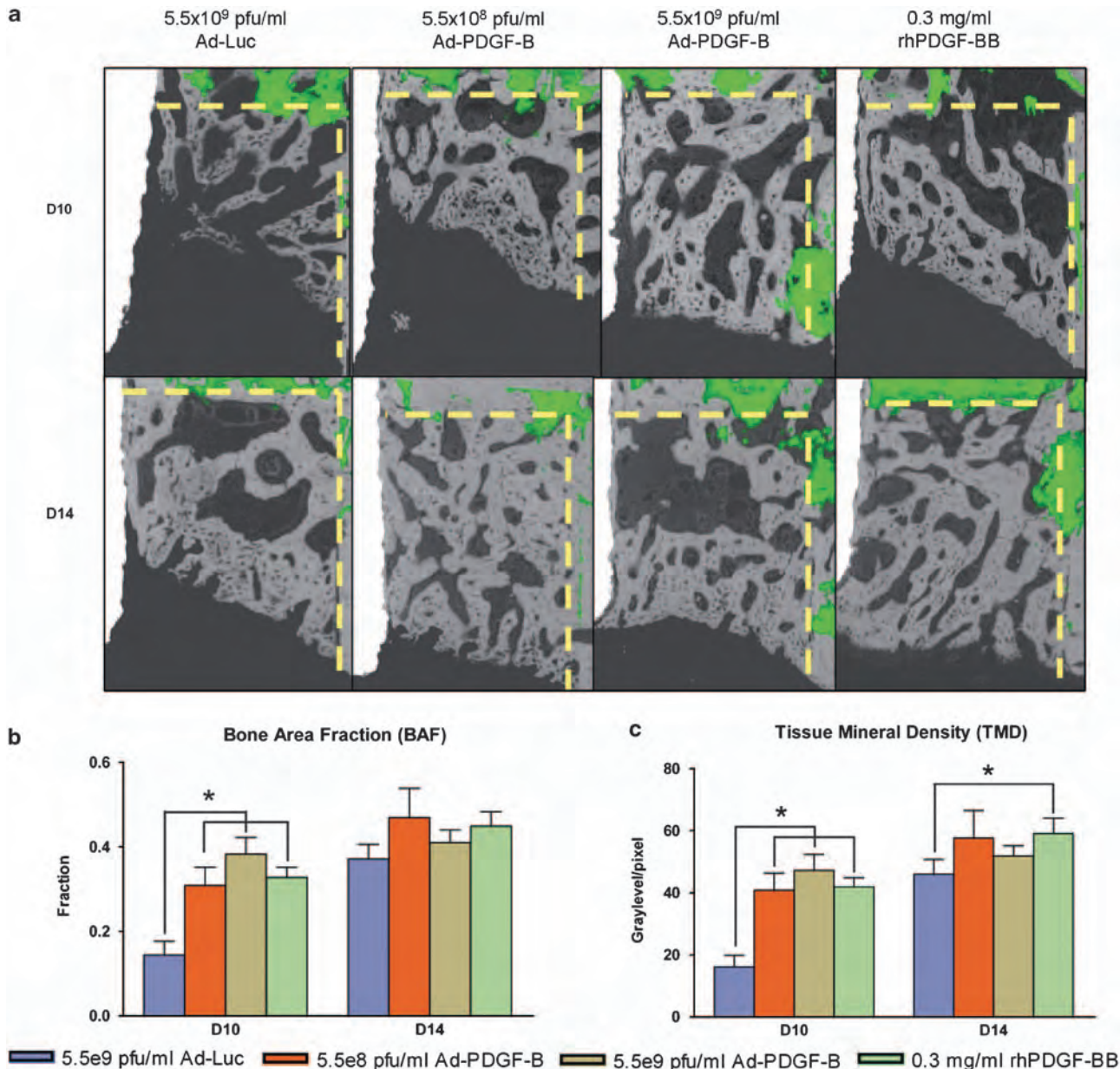
Received 13 April 2009; revised 23 June 2009; accepted 23 June 2009; published online 10 September 2009



**Figure 1** Histological view of each group for 10 and 14 days (a) and two-dimensional evaluations; bone-to-implant contact (BIC) (b) and defect fill (c). (a) Histological images were overlapped by fluorescent images made by calcein injection 3 days after surgery. The fluorescence indicates the original defect boundaries. The results of Ad-Luc defects shows sparse bone formation at day 10 and a lesser degree of bone maturation at 10 and 14 days. All the PDGF-related specimens showed increased new bone formation at 10 and 14 days compared with the Ad-Luc group. Scale bar = 200  $\mu$ m (top right panel), original magnification,  $\times$ 40. (b) In BIC analysis,  $5.5 \times 10^9$  pfu ml<sup>-1</sup> Ad-PDGF-B and rhPDGF-BB groups showed significantly higher ratio than the control group at 10 days, and  $5.5 \times 10^9$  pfu ml in top right panel represents Ad-PDGF-B showed significantly higher ratio than the control group at 14 days. (c) In defect fill analysis, all three PDGF treatment groups showed higher fractions than Ad-Luc-treated defects at 10 and 14 days. Black area in left side: dental implant; black asterisks: matured new bone; red asterisks: young new bone; and dashed line: borders of the osseous defect. Data are presented as mean and bars indicate standard error measurement ( $n = 6-8$ ). \* $P < 0.05$ , \*\* $P < 0.01$ , Abbreviation: BIC: bone to implant contact.

primary trabecular bone were noted at the coronal margin (red asterisks) in Ad-Luc-treated specimens, and thicker bone trabeculae and defect fill (DF) were evident in all PDGF-treated specimens (black asterisks in  $5.5 \times 10^8$  and  $5.5 \times 10^9$  pfu ml<sup>-1</sup> Ad-PDGF-B, and rhPDGF-BB). Also at day 14, more mature bone apposition and near-complete DF were noted for all PDGF-treated specimens (Figure 1a, lower panel). The histomorphometric measurements of the  $5.5 \times 10^9$  pfu ml<sup>-1</sup> Ad-PDGF-B and rhPDGF-BB groups showed significantly higher bone-implant contact (BIC)

than the Ad-Luc group at day 10 ( $P < 0.05$ , Figure 1b). Furthermore, all PDGF groups indicated higher DF than the Ad-Luc group at days 10 ( $P < 0.01$ , Figure 1c) and 14 ( $P < 0.05$ , Figure 1c). An equivalent defect repair pattern was noted from the backscattered scanning electron microscopy (BS-SEM) images (Figure 2a). At day 10, BS-SEM measurements also showed a significant difference among all PDGF-treated groups compared with the Ad-Luc-treated group in both bone-area fraction (BAF,  $P < 0.05$ , Figure 2b) and tissue mineral density (TMD,  $P < 0.05$ ,



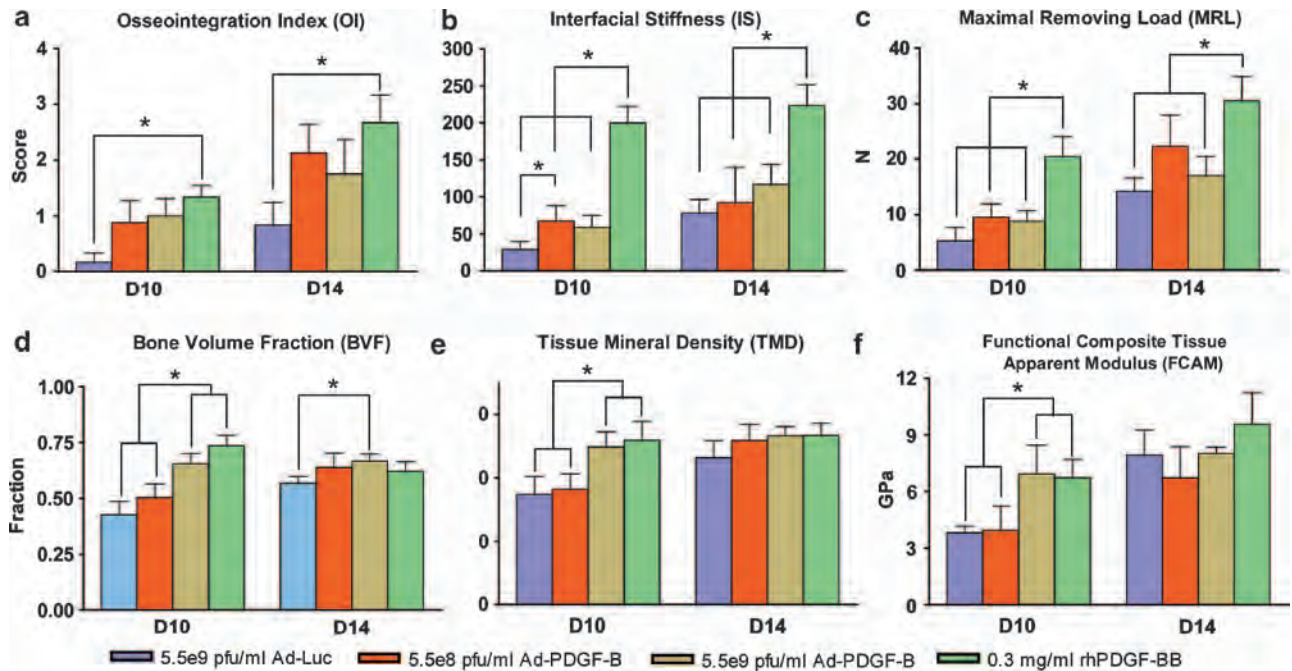
**Figure 2** Backscattered SEM (BS-SEM) images (a) and two-dimensional evaluations, bone-area fraction (b), and tissue mineral density (c). (a) BS-SEM images were merged with fluorescent images (dashed line: borders of the osseous defect). The BS-SEM images show mineralized tissue against the oral implant surface. (original magnification,  $\times 42$ ) (b) The three PDGF treatment groups showed a significant difference in bone area fraction at 10 days compared with the control group. (c) The three PDGF groups also showed significant differences in tissue mineral density at 10 days and the rhPDGF-BB group showed significance at 14 days compared with Ad-Luc defects. Data are presented as mean and bars indicate standard error measurement ( $n = 6-8$ ).  $*P < 0.05$ .

Figure 2c). A significant difference between rhPDGF-BB and Ad-Luc groups in TMD was also noted at day 14 ( $P < 0.05$ , Figure 3c). Completion of the DF was noted in all the animals by day 21, and no significant differences for any BS-SEM or histomorphometric parameters could be found among all the groups (data not shown).

#### Both Ad-PDGF-B and rhPDGF-BB promote osseointegration

The consequence of push-out testing was reflected from the osseointegration index (OI), with all PDGF-treated specimens showing higher scores than Ad-Luc, with

significant differences noted between rhPDGF-BB and Ad-Luc at both days 10 and 14 ( $P < 0.05$ , Figure 3a). PDGF application tended to improve the interfacial stiffness (IS) and maximum removal loading (MRL) compared with the Ad-Luc group. The rhPDGF-BB treatment indicated significantly higher IS than all other groups at days 10 and 14 ( $P < 0.05$ , Figure 3b), and higher MRL than all other groups at day 10 ( $P < 0.05$ , Figure 3c). At day 14, the MRL of rhPDGF-BB was significantly higher compared with both the Ad-Luc and the  $5.5 \times 10^9$  pfu ml<sup>-1</sup> Ad-PDGF-B groups ( $P < 0.05$ , Figure 3c). Significant improvement of IS using  $5.5 \times 10^8$  pfu ml<sup>-1</sup> Ad-PDGF-B treatment versus Ad-Luc ( $P < 0.05$ , Figure 3b)



**Figure 3** Biomechanical and micro-CT/functional stimulations show that Ad-PDGF-B and PDGF-BB improve osseointegration *in vivo*. Osseointegration index (a), interfacial stiffness (b), and maximum removing load (c) showed significant differences between rhPDGF-BB treatment and the other three groups. Bone volume fractions (d), tissue mineral density (e) and functional tissue modulus (f) show that  $5.5 \times 10^9$  pfu ml<sup>-1</sup> Ad-PDGF-B and rhPDGF-BB groups showed significant differences compared with the  $5.5 \times 10^8$  pfu ml<sup>-1</sup> AD-PDGF-B and Ad-Luc groups. There were no significant differences in tissue mineral density and functional composite tissue apparent modulus (FCAM) at day 14. Data are presented as mean and bars indicate standard error measurement ( $n = 6-8$ ). \* $P < 0.05$ .

was also seen at day 10. Most day 21 specimens experienced cortical bone fractures during the push-out testing (suggestive of strong osseointegration), and no significant differences among all the groups in IS and OI scores were noted (data not shown).

Micro-computed tomography (micro-CT) images were analyzed after implant removal, and both the  $5.5 \times 10^9$  pfu ml<sup>-1</sup> Ad-PDGF-B and rhPDGF-BB groups showed significantly higher bone volume fraction (BVF) and TMD than the  $5.5 \times 10^8$  pfu ml<sup>-1</sup> Ad-PDGF-B and Ad-Luc groups at day 10 ( $P < 0.05$ , Figure 3d and e). A significant difference in BVF was found between  $5.5 \times 10^9$  pfu ml<sup>-1</sup> Ad-PDGF-B and Ad-Luc groups at day 14 ( $P < 0.05$ , Figure 3d). Both the  $5.5 \times 10^9$  pfu ml<sup>-1</sup> Ad-PDGF-B and rhPDGF-BB groups showed equivalent extents of functional composite tissue apparent modulus (FCAM), which was significantly stiffer than the  $5.5 \times 10^8$  pfu ml<sup>-1</sup> Ad-PDGF-B or Ad-Luc group at day 10 ( $P < 0.05$ , Figure 3f). At day 14, there were no FCAM differences between any of the treatment groups.

**Local delivery of Ad-PDGF-B shows acceptable safety profiles *in vivo***

In a separate study of systemic safety, animals were treated with collagen alone (control) or collagen containing Ad-PDGF-B ( $5.5 \times 10^8$  or  $5.5 \times 10^9$  pfu ml<sup>-1</sup>). Blood samples were taken at various time points for hematological and clinical chemistry analyses and PCR analysis for vector sequence. All animals survived until the day of killing, with no progressive swelling or symptoms noted.

The majority of hematological and clinical chemistry parameters were within their normal ranges with no significant differences between Ad-PDGF-B and collagen-only treatments (Tables 1 and 2).

Vector-specific quantitative PCR<sup>6</sup> was carried out on blood samples taken at baseline, days 1, 2, 3, 4, 5, 7, 14, 21, 28, and 35 after treatment. Ad-PDGF-B was not detected in the bloodstream over the 35-day observation period (data not shown).

**Discussion**

This study shows that both Ad-PDGF-B gene and rhPDGF-BB protein delivery promote the acceleration of neo-osteogenesis of peri-implant bony defects *in vivo*. The effect on bone apposition was examined through DF from histomorphometry (Figure 1c), BAF from BS-SEM (Figure 2b) and BVF from micro-CT (Figure 3d). From these results, all treatment groups, especially the  $5.5 \times 10^9$  pfu/ml Ad-PDGF-B and rhPDGF-BB groups, showed significantly greater bone formation compared with the Ad-Luc vector control group at 10 days. Regarding bone maturation, the Ad-Luc-treated defects showed sparse and limited new bone formation and slower bone formation within the defect area compared with the other three groups. By day 14, in the Ad-Luc group, new bone near the base of the defect (Figure 1a) showed thick trabeculae and bone marrow formation, suggesting greater maturation, whereas the thin trabeculae and primary woven bone-like structures at the coronal portion of the defects suggests early-stage

**Table 1** Hematological analyses for Ad-PDGF-B delivery<sup>a</sup>

Hematological parameters	Before surgery			Day 3			Day 7			Day 14		
	Col	L-Ad	H-Ad	Col	L-Ad	H-Ad	Col	L-Ad	H-Ad	Col	L-Ad	H-Ad
	WBC (K $\mu\text{l}^{-1}$ )	11.87 (2.99)	10.55 (1.58)	12.15 (2.69)	9.67 (2.82)	11.04 (1.49)	11.81 (1.67)	14.70 (5.22)	11.97 (4.44)	12.15 (2.78)	10.90 (3.98)	11.36 (3.02)
Neutrophil (K $\mu\text{l}^{-1}$ )	2.988 (0.909)	2.462 (0.914)	3.512 (0.995)	2.807 (1.161)	4.542 (1.397)	3.323 (0.778)	4.438 (1.994)	4.340 (2.913)	3.887 (0.878)	3.343 (1.600)	4.547 (2.489)	3.527 (1.272)
Lymphocyte (K $\mu\text{l}^{-1}$ )	8.160 (1.355)	7.487 (0.699)	7.840 (1.511)	6.452 (2.962)	5.943 (0.918)	7.768 (1.391)	9.400 (3.051)	6.905 (1.234)	7.658 (2.086)	6.933 (2.103)	6.162 (0.785)	7.988 (1.845)
Monocyte (K $\mu\text{l}^{-1}$ )	0.635 (0.311)	0.560 (0.139)	0.550 (0.179)	0.305 (0.091)	0.488 (0.128)	0.648 (0.147)	0.643 (0.299)	0.707 (0.128)	0.493 (0.307)	0.537 (0.307)	0.593 (0.227)	0.540 (0.147)
Eosinophil (K $\mu\text{l}^{-1}$ )	0.073 (0.039)	0.048 (0.019)	0.190 (0.158)	0.100 (0.082)	0.098 (0.034)	0.057 (0.028)	0.165 (0.128)	0.157 (0.224)	0.102 (0.122)	0.085 (0.060)	0.048 (0.018)	0.160 (0.118)
Basophil (K $\mu\text{l}^{-1}$ )	0.007 (0.012)	0.003 (0.005)	0.052 (0.064)	0.015 (0.023)	0.015 (0.023)	0.007 (0.010)	0.055 (0.053)	0.035 (0.067)	0.002 (0.004)	0 (0)	0.007 (0.010)	0.013 (0.014)
RBC (M $\mu\text{l}^{-1}$ )	8.713 (0.305)	8.315 (0.405)	7.388 (0.783)	8.033 (0.585)	8.300 (0.893)	8.082 (0.449)	7.558 (0.493)	7.502 (0.329)	7.925 (0.344)	7.277 (1.257)	7.933 (0.701)	7.963 (0.492)
Hb (g per 100 ml)	16.03 (0.56)	15.53 (0.40)	15.20 (0.64)	15.05 (0.62)	15.13 (1.72)	14.63 (0.78)	13.85 (1.07)	13.65 (0.46)	14.38 (0.58)	14.37 (1.86)	15.68 (1.42)	14.67 (0.23)
Hct (%)	51.68 (2.22)	48.27 (2.76)	42.97 (4.51)	47.50 (3.68)	48.03 (4.88)	47.88 (2.31)	45.02 (3.14)	43.60 (1.71)	47.32 (1.88)	43.95 (8.27)	46.77 (4.35)	48.23 (2.15)
MCV (fl)	59.33 (2.25)	58.07 (1.47)	58.18 (1.64)	59.13 (2.29)	57.90 (1.45)	59.30 (1.43)	59.58 (2.23)	58.20 (0.85)	59.72 (1.59)	60.25 (2.48)	58.97 (2.05)	60.65 (1.72)
MCH (pg)	18.42 (0.74)	18.70 (0.87)	20.77 (2.30)	18.78 (0.89)	18.27 (1.16)	18.13 (0.64)	18.33 (1.14)	18.23 (0.74)	18.13 (0.55)	19.92 (1.40)	19.77 (0.38)	18.47 (1.18)
MCHC (g per 100 ml)	31.05 (0.94)	32.25 (1.59)	35.68 (3.79)	31.75 (1.47)	31.52 (1.64)	30.53 (0.55)	30.77 (1.07)	31.30 (1.07)	30.40 (0.26)	33.12 (2.95)	33.55 (0.81)	30.47 (1.49)
RDW (%)	14.05 (0.42)	13.97 (0.53)	14.10 (0.57)	14.23 (0.49)	14.25 (0.72)	14.10 (0.64)	15.27 (0.72)	15.05 (0.88)	14.50 (0.59)	15.90 (0.43)	15.77 (0.55)	15.55 (0.38)

Abbreviations: Col, collagen matrix only group; Hb, hemoglobin; Hct, hematocrit; L-Ad,  $5.5 \times 10^8$  pfu  $\text{ml}^{-1}$  Ad-PDGF-B-treated group; H-Ad,  $5.5 \times 10^8$  pfu  $\text{ml}^{-1}$  Ad-PDGF-B-treated group; MCH, mean corpuscular hemoglobin; MCHC, mean corpuscular hemoglobin concentration; MCV, mean corpuscular volume; RDW, red blood cell distribution width; RBC, red blood cell; WBC, white blood cell.  
<sup>a</sup>All comparisons to the collagen group ( $n = 6$  per group). The number in this table shows the average value of parameters from the each group and the number in the parentheses refers to the standard deviations. Neither significant differences nor value out of normal range were noted among the Ad-PDGF-B and collagen matrix groups during early time points, as well as beyond 14 days (data not shown).

**Table 2** Clinical chemical analyses for Ad-PDGF-B delivery<sup>a</sup>

Clinical chemical parameters	Before surgery			Day 3			Day 7			Day 14		
	Col	L-Ad	H-Ad	Col	L-Ad	H-Ad	Col	L-Ad	H-Ad	Col	L-Ad	H-Ad
	Albumin (g per 100 ml)	2.900 (0.200)	3.100 (0.210)	2.750 (0.055)	2.733 (0.216)	2.783 (0.223)	2.917 (0.223)	2.667 (0.216)	2.600 (0.126)	2.917 (0.117)	2.750 (0.243)	2.700 (0.420)
ALP (U $\text{l}^{-1}$ )	200.67 (29.49)	253.50 (28.81)	207.50 (36.30)	183.67 (45.70)	195.50 (45.05)	141.17 (30.64)	177.83 (41.80)	163.50 (28.39)	192.17 (40.63)	204.00 (46.43)	227.83 (51.34)	200.00 (36.78)
ALT (U $\text{l}^{-1}$ )	89.67 (7.74)	88.17 (6.68)	90.33 (8.55)	75.00 (8.60)	76.67 (13.31)	69.50 (3.78)	87.50 (22.82)	85.50 (7.23)	89.83 (15.96)	85.83 (10.46)	78.83 (8.11)	89.67 (11.27)
Amylase (U $\text{l}^{-1}$ )	2182.17 (119.59)	2054.5 (333.84)	2019.67 (209.93)	1706.67 (256.08)	1335.00 (246.33)	1487.50 (155.96)	1779.00 (189.74)	1589.50 (232.52)	1764.17 (188.13)	1893.17 (226.83)	1742.00 (504.32)	1945.67 (219.46)
AST (U $\text{l}^{-1}$ )	81.33 (16.67)	78.33 (9.42)	80.83 (12.95)	91.50 (12.42)	115.00 (42.68)	88.33 (17.10)	97.83 (23.70)	71.50 (10.88)	98.00 (11.51)	73.00 (9.38)	85.50 (10.58)	83.50 (14.15)
Bilirubin (mg per 100 ml)	19.67 (1.37)	21.83 (1.47)	23.33 (1.86)	23.33 (2.25)	24.00 (1.67)	20.67 (1.03)	21.67 (1.63)	19.33 (1.03)	22.83 (1.47)	21.67 (1.86)	29.67 (14.60)	22.33 (2.07)
Calcium (mg per 100 ml)	11.18 (0.70)	10.78 (0.23)	10.63 (0.15)	10.28 (0.16)	10.32 (0.23)	10.60 (0.23)	10.47 (0.22)	10.57 (0.29)	10.35 (0.25)	10.52 (0.22)	10.58 (0.26)	10.80 (0.27)
Cholesterol (mg per 100 ml)	87.17 (17.97)	87.50 (13.07)	81.00 (7.69)	99.33 (14.31)	106.83 (13.12)	95.33 (7.31)	83.00 (20.95)	83.83 (9.81)	82.33 (7.45)	90.50 (17.07)	93.17 (16.10)	84.33 (15.34)
Creatine kinase (U $\text{l}^{-1}$ )	105.83 (11.86)	94.67 (12.04)	104.50 (36.54)	426.5 (72.45)	403.50 (146.06)	153.00 (119.30)	302.50 (132.63)	115.67 (55.85)	346.33 (117.08)	83.50 (35.80)	244.83 (110.49)	94.83 (22.48)
Creatinine (mg per 100 ml)	0.283 (0.041)	0.383 (0.041)	0.383 (0.041)	0.383 (0.041)	0.400 (0.063)	0.333 (0.082)	0.433 (0.234)	0.367 (0.052)	0.400 (0)	0.350 (0.055)	1.700 (3.184)	0.400 (0)
Glucose (mg per 100 ml)	181.00 (18.98)	187.33 (3.44)	283.33 (52.30)	225.17 (48.06)	251.00 (77.69)	226.33 (39.62)	243.17 (127.82)	275.83 (33.58)	209.83 (23.20)	255.83 (58.81)	223.83 (62.07)	295.83 (40.92)
Phosphorus (mg per 100 ml)	5.983 (0.313)	5.767 (0.497)	5.300 (0.498)	5.567 (0.383)	5.533 (0.524)	5.700 (0.704)	5.733 (0.625)	5.250 (0.367)	5.983 (0.417)	5.700 (0.228)	6.500 (1.942)	5.467 (0.372)
T. bilirubin (mg per 100 ml)	0.167 (0.052)	0.117 (0.041)	0.167 (0.082)	0.117 (0.041)	0.217 (0.240)	0.400 (0.642)	0.250 (0.207)	0.167 (0.103)	0.183 (0.075)	0.200 (0.155)	0.150 (0.122)	0.217 (0.117)
Total protein (g per 100 ml)	6.517 (0.256)	6.550 (0.217)	6.017 (0.117)	6.217 (0.343)	6.267 (0.344)	6.467 (0.484)	6.233 (0.207)	5.850 (0.207)	6.300 (0.141)	6.183 (0.204)	6.150 (0.689)	6.067 (0.314)
Globulin (g per 100 ml)	3.617 (0.407)	3.483 (0.041)	3.283 (0.147)	3.467 (0.186)	3.483 (0.133)	3.567 (0.273)	3.533 (0.695)	3.250 (0.152)	3.400 (0.632)	3.383 (0.117)	3.560 (0.114)	3.300 (0.141)

Abbreviations: ALP, alkaline phosphatase; ALT, alanine transaminase; AST, aspartate transaminase; Col, collagen matrix only group; L-Ad,  $5.5 \times 10^8$  pfu  $\text{ml}^{-1}$  Ad-PDGF-B-treated group; H-Ad,  $5.5 \times 10^8$  pfu  $\text{ml}^{-1}$  Ad-PDGF-B-treated group; T. bilirubin, total bilirubin.  
<sup>a</sup>All comparisons to the collagen group ( $n = 6$  per group). The number in this table shows the average value of parameters from the each group and the number in the parentheses refers to the standard deviations. Neither significant differences nor value out of normal range were noted among the Ad-PDGF-B and collagen matrix groups during early time points, as well as beyond 14 days (data not shown).

osteogenesis. However, in all PDGF-treated groups, advanced bone maturation throughout the defect area, especially in the higher dose Ad-PDGF-B and rhPDGF-BB groups, indicates that new bone formation initiated earlier in those two groups compared with controls. Taken together, these results strongly suggest that PDGF delivery, through both the protein and the gene transfer vector, significantly accelerated and enhanced new bone formation in the peri-implant defects, and the higher dose of Ad-PDGF-B showed more favorable results than lower dosage, suggesting a dose-dependent effect on osseointegration.

We also presented FCAM predicting the functional contribution of the newly-formed bone through the FE optimization procedures.<sup>15</sup> It is more correlated with the implant interfacial resistance than any single structural parameter. Significantly, higher FCAM from the  $5.5 \times 10^9$  pfu ml<sup>-1</sup> Ad-PDGF-B and rhPDGF-BB treatment groups at day 10 indicates that both PDGF protein and gene delivery stimulate not only osteogenesis but also favorable initial implant function.

Two- and three-dimensional quantification results between rhPDGF-BB and higher dose Ad-PDGF-B were also comparable (Figures 1–3). However, the biomechanical analyses did not show equivalent trends, whereas rhPDGF-BB showed significant improvements compared with Ad-Luc for most of the parameters (Figure 3a–c). Although the correlation between implant stability and peri-implant structures had been proven in previous research,<sup>16,17</sup> this finding may be due to the different delivery profile of PDGF by either Ad or as a protein. Although the initial response to a bolus administration of rhPDGF-BB may be robust, the protein's short half-life results in rapid degradation within a few days,<sup>2</sup> and a decrease in the mitogenic response. In contrast, Ad-PDGF-B delivery shows a delayed PDGF-BB expression profile that gradually decreases to ~20% of the highest level by day 14 *in vivo*.<sup>14</sup> This finding is consistent with a previous report whereby Ad-PDGF-B prolongs PDGF signaling, leading to a delay with respect to timing of osteogenic differentiation.<sup>18</sup>

The effects of PDGF on osseous wound healing have been reported mechanistically in previous investigations. It had been shown that PDGF signaling is important for chemotaxis and proliferation of osteoblasts and fibroblasts.<sup>19,20</sup> However, PDGF's ability to induce osteogenic lineage differentiation is less clear. Tokunaga *et al.*<sup>21</sup> reported that PDGFR $\beta$  signaling strongly inhibited osteogenic differentiation of mesenchymal stem cells, and Kono *et al.*<sup>22</sup> further validated that the Erk signaling, which is the subsequent PDGFR pathway, negatively regulated osteogenesis. On the other hand, other evidence implies that PDGF contributes to osteogenic differentiation through a more downstream mechanism. Huang *et al.*<sup>23</sup> detected PDGF mRNA expression at both the early proliferation stage and a late differentiation stage of osteoprogenitor cells. Furthermore, Ng *et al.*<sup>24</sup> showed that PDGFR activation was a key step for the osteogenic lineage differentiation of mesenchymal stem cells, whereas inhibition of PDGFR $\beta$  resulted in decreased mineralized nodule formation. Kratchmarova *et al.*<sup>25</sup> reported that PDGF increased new bone formation *in vivo* despite limited influences in osteogenic differentiation *in vitro*. These results imply that the differentiation is promoted at a certain level of expression, such as

dose- or time-dependent reactions.<sup>19,20</sup> De Donatis *et al.*<sup>19</sup> reported that a higher concentration of PDGF is favorable for mitogenesis and lower doses for cell motility. Hsieh and Graves<sup>20</sup> found that pulse application of PDGF enhances bone formation, but prolonged exposure to PDGF limited *in vitro* bone regeneration. As osteogenesis involves a cascade of events *in vivo*, varying strategies of PDGF delivery must be considered for different indications. Thus, the rhPDGF-BB treatment may be suitable for the needs of rapid bone fill, where it would quickly recruit cells without significantly affecting the time frame of subsequent differentiation (Supplementary Figure 1a). The higher dose of Ad-PDGF-B may be a better choice for a large wound site (that remains to be tested), in which the sustained PDGF signal would attract cell progenitors for a more extended, but still limited period of time so that the differentiation and maturation would initiate after PDGF signaling subsided (Supplementary Figure 1b). Given the limited size of the rat maxilla and the high cell proliferative activity, it is necessary to further validate this assumption in a large animal model with more challenging, critical-size defects.

This use of gene therapy introduced a different strategy when compared with traditional scaffold-growth factor delivery. In our approach, the main function of the gene-activated matrix (that is, collagen matrix) was to mobilize the vector and allow for cell invasion.<sup>26</sup> The vector is then actively transfected into the cells, followed by disintegration of capsid, condensed by the adenovirus core proteins to enter the nucleus (<40 nm diameter) for the subsequent expression of the carrier gene.<sup>27</sup> Thus, the rate-limiting step of gene delivery was the vector transduction. High levels of adenovirus transduction within the first 2 weeks of delivery, and favorable regenerative effects have been documented in several studies.<sup>6,14,28</sup> Further efforts on the condensation of adenovirus vector may be beneficial for amplifying the efficiency of the gene therapy.<sup>27</sup>

The angiogenic effect of PDGF, which are similar to the effect of vascular endothelial growth factor, may also be favorable for osseous wound repair. During wound healing, angiogenesis is an important event for new tissue regeneration (that is, providing nutrients and essential signals). The PDGFs have a similar structure to vascular endothelial growth factor,<sup>29</sup> and PDGF-BB enhances fibroblast growth factor-2 stimulated vascular endothelial growth factor release.<sup>30</sup> PDGFR $\beta$  also has an important role in angiogenesis.<sup>31</sup> Therefore, it is reasonable to conclude that PDGF-BB also positively affects angiogenesis and ultimately contributes to bone formation. Considering that dental implant function (with a metallic non-vascularized interface) is largely dependent on the surrounding bone quantity, quality and the wound healing microenvironment, these accelerating and enhancing bone formation effects of PDGF may promote greater bone volume for earlier implant placement and loading.

One important consideration with the use of gene therapy vectors is the potential immune response and related sequelae.<sup>32,33</sup> In our study, Ad-PDGF-B was delivered in a collagen matrix, which potentially masks the host immune function against Ad vectors *in vivo*.<sup>28,18,26,34</sup> Typically, transformation and self-replication is eliminated by removing the E1- and E3-gene regions of the adenovirus genome.<sup>35</sup> We discovered no

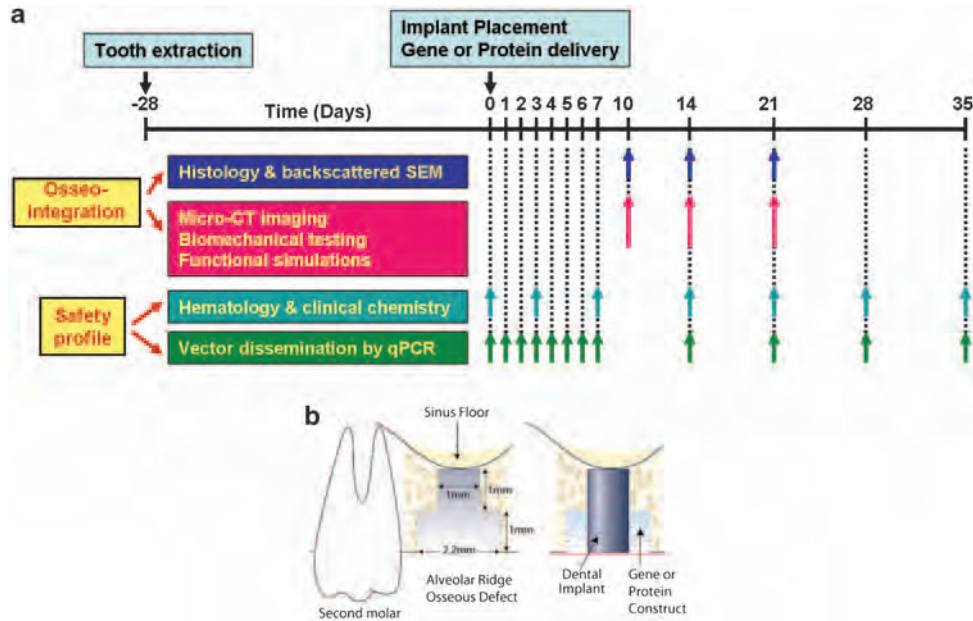


**Figure 4** Experimental design (a) and experimental model illustration (b). Implant surgery was performed 4 weeks following maxillary first molar extraction. To create a consistent and reproducible defect, custom-made step drills were used. After dental implant placement, the bone defect was filled with  $5.5 \times 10^9$  pfu ml<sup>-1</sup> Ad-Luc,  $5.5 \times 10^8$  pfu ml<sup>-1</sup> Ad-PDGF-B,  $5.5 \times 10^9$  pfu ml<sup>-1</sup> Ad-PDGF-B or 0.3 mg ml<sup>-1</sup> rhPDGF-BB formulated with the collagen matrix for evaluating osseointegration ( $n=6-8$  per group per time point). Histomorphometric and BS-SEM measurements were done at days 10, 14 and 21 after implant installation, and three-dimensional evaluations (micro-CT imaging) as well as functional assessments (biomechanical testing and functional simulations) were done at days 10, 14 and 21 after implant installation. For evaluating the safety profile, the bone defect was filled with  $5.5 \times 10^8$  pfu ml<sup>-1</sup> Ad-PDGF-B,  $5.5 \times 10^9$  pfu ml<sup>-1</sup> Ad-PDGF-B or collagen matrix alone. The hematology, chemical chemistry and vector dissemination were evaluated over a period of 35 days ( $n=6$  per group per time point).

significant vector dissemination or alteration of hematological and clinical chemistry parameters. Our results showed a favorable preclinical safety profile and was comparable with our previous investigation examining Ad-PDGF-B in periodontal defects.<sup>6</sup> Furthermore, a non-viral-based vector might be an alternative for delivering the PDGF-B gene with minimal safety concerns. However, further efforts on the improvement of efficient delivery and expression of the non-viral vectors is still necessary.<sup>36,37</sup>

In summary, this investigation indicates the first reported use of Ad-PDGF-B administration to promote alveolar bone repair and osseointegration in alveolar ridge defects. These findings suggest that Ad-PDGF-B stimulates osseointegration that is comparable with the delivery of PDGF-BB protein. A good safety profile was shown supportive for extending this approach to large animal model studies examining large critical-size bony defects in the craniofacial complex.

## Materials and methods

### Experimental design

A total of 100 male Sprague–Dawley rats were used in this study and the general timeline is shown in Figure 4a. On the basis of the power analysis calculations from a similar study, 6–8 animals were analyzed per treatment per time point.<sup>14</sup> A rat dental implant osseointegration wound model was modified for the *in vivo* experiments. A total of 82 animals were used for evaluating the effects of osseointegration, with three time points (days 10, 14

and 21) and four treatment groups ( $5.5 \times 10^9$  pfu ml<sup>-1</sup> Ad-Luc as the control group,  $5.5 \times 10^8$  pfu ml<sup>-1</sup> Ad-PDGF-BB,  $5.5 \times 10^9$  pfu ml<sup>-1</sup> Ad-PDGF-BB and 0.3 mg ml<sup>-1</sup> rhPDGF-BB) evaluated. In addition, 18 animals were equally divided into three treatment groups (collagen matrix alone as the control group,  $5.5 \times 10^8$  pfu ml<sup>-1</sup> Ad-PDGF-BB and  $5.5 \times 10^9$  pfu ml<sup>-1</sup> Ad-PDGF-BB) and used for determining the preclinical safety profile, with assessments performed on these same animals over an observation period of 35 days.

### Ad vectors and recombinant protein

Ad-PDGF-B (E1-, E3-deleted adenovirus serotype 5 encoding human platelet-derived growth factor-B) and Ad-Luc (E1-, E3-deleted adenovirus serotype 5 encoding firefly luciferase) have been previously described.<sup>6</sup> In both vectors, transgene expression is under control of the CMV promoter. Titers of virus stocks were determined on embryonic kidney 293 cells by plaque assay and expressed as the particle number per milliliter.<sup>7</sup> The rhPDGF-BB was purchased from Biomimetic Therapeutics Inc. (Franklin, TN, USA) at a working concentration of 0.5 mg ml<sup>-1</sup>.

### Preparation of vector/protein-gene activated matrix

Ad-PDGF-B, Ad-Luc and rhPDGF-BB were dialyzed into GTS buffer (2.5% glycerol, 25 mM NaCl, 20 mM Tris, pH 8.0) and formulated in bovine fibrillar type I collagen matrix (Matrix Pharmaceutical Inc., Fremont, CA, USA) at a final concentration of 2.6%.

### Animal model for evaluating therapeutic effects

All animal procedures followed the guidelines from the Committee on Use and Care of Animals of the University of Michigan. The maxillary first molars were extracted bilaterally 4 weeks before dental implant installation. After healing, an osteotomy was created using a custom drill-bit by a single surgeon (Y-JS). The drill-bit was designed with a 0.95-mm diameter, 1 mm long-apical portion and a 2.2-mm diameter, 1 mm long at the coronal aspect (Figure 4b). The apical part of the drill created an osteotomy for initial fixation and the coronal part of the drill created a circumferential osseous defect before dental implant installation. A custom cylinder-type titanium mini-implant (kind gift of Institut Straumann AG, Basel, Switzerland), 1 mm in diameter and 2 mm in depth, was press-fit into the surgically created socket (Figure 4b). The remaining defect was then filled with the type I collagen matrix containing  $5.5 \times 10^9$  pfu ml<sup>-1</sup> Ad-Luc,  $5.5 \times 10^8$  pfu ml<sup>-1</sup> Ad-PDGF-B,  $5.5 \times 10^9$  pfu ml<sup>-1</sup> Ad-PDGF-B or 0.3 mg ml<sup>-1</sup> rhPDGF-BB (Figure 4b). Ad-Luc has not previously exhibited biological activities in dentoalveolar defects<sup>14</sup> and served as a control group in this study. The surgical area was covered by gingival tissue and re-approximated using butyl cyanoacrylate (Periacryl, Glustitch Inc., Point Roberts, WA, USA). The vital fluorochrome dye, calcein (10 mg kg<sup>-1</sup>), was injected intramuscularly after 3 days, and antibiotics (268 mg l<sup>-1</sup> ampicillin in 5% dextrose water) were provided during the first 7 days after operation.

### BS-SEM and histology

Coded maxillae containing the implants were harvested upon killing, with one side of maxillae taken for BS-SEM and histology, whereas the contralateral maxillae were used for biomechanical assessments (see following section). The specimens were fixed in 50% ethanol for at least 72 h and subsequently embedded in epoxy resin. The specimens were then sectioned in the longitudinal direction relative to the implants using a diamond saw blade (Crystalite Co., Westerville OH, USA), then polished to achieve a 50- to 100- $\mu$ m final thickness. The tissue mineralization was evaluated under the back-scattered mode on Qanta F1B SEM with  $\times 45$  magnification, calibrated with aluminum and carbon discs,<sup>38</sup> and transferred to physical density using bone substitute radiographic phantoms (Gammex Inc., Middleton WI, USA). The photographs were then segmented and thresholded by Otsu's adaptive technique.<sup>39</sup> To eliminate any metal scattering effect, the measured bone-implant interface was defined as the horizontal distance 5  $\mu$ m from the outermost homogenous high-intensity area. The defect borders were projected using the calcein fluorescent images. BAF (the ratio of newly formed bone in the defect to the entire defect area) and TMD within the defect (the average grayscale level of mineralized tissue within the defect area) were measured from BS-SEM images. Next, histological staining by methylene blue was performed, with the acid fuchsin used as the counterstain.<sup>28</sup> BIC (the ratio of the length of bone contacting the titanium to the entire length of titanium interface with the defect area) and DF (the ratio of bone-occupied area to the entire defect area) were measured by calibrated examiners P-CC and Y-JS).

### Biomechanical, three-dimensional radiographic and functional evaluations

The remaining maxillae were used for biomechanical and micro-CT evaluation and stored in normal saline at  $-20^\circ\text{C}$  to preserve the mechanical integrity. After thawing at room temperature, the specimens were rapidly secured in acrylic resin. The mini-implants were meticulously pushed out of each maxilla using an MTS machine (Model 858, Mini-Bionix II, MTS Systems Corp., Eden Prairie, MN, USA) at a constant displacement rate of 0.1 mm s<sup>-1</sup>, while recording the load-displacement relationship of the top of implant during the push-out procedures. The region from 20 to 80% of the MRL was chosen and a linear regression was performed to calculate the IS. A previously described OI based on the nature of the bone fail during implant push-out tests was also used to further document the interfacial biomechanical behavior (Supplementary Table S1).<sup>15</sup>

After implant push-out, micro-CT scans were performed using an eXplore Locus SP Micro-CT system (GE HealthCare, London, ON, Canada) and reconstructed to the voxel size of 18  $\mu\text{m} \times 18 \mu\text{m} \times 18 \mu\text{m}$ . The spatial relationship of the mini-implant and surrounding tissues was then analyzed using a customized MATLAB (Mathworks Inc., Natick, MA, USA) algorithm. The images were segmented with a threshold determined by Otsu's adaptive technique,<sup>39</sup> and several parameters were quantitatively evaluated within the osseous defect areas: (1) BVF: the volume of mineralized tissue within the osseous wound divided by the volume of osseous wound; (2) TMD: the mineral content of the radiographic-defined mineralized tissue within the osseous wound divided by the volume of osseous wound; (3) bone mineral density: the mineral density within the radiographic-defined mineralized tissue in the osseous wound. After micro-CT evaluations, the images were transferred to create a finite element (FE) mesh, and the functional bone modulus (referring to the rigidity of bone within the area of interest toward dental implant) and FCAM (rigidity of the whole tissue within the area of interest toward dental implant) were generated from previously described simulation procedures.<sup>15</sup>

### Safety profile determination

A total of 18 male Sprague-Dawley rats had their first maxillary molars extracted, osseous defect created and implant placement as previously described.<sup>28</sup> The osseous defects were filled with the type I collagen vehicle alone, or containing Ad-PDGF-B ( $5.5 \times 10^8$  or  $5.5 \times 10^9$  pfu ml<sup>-1</sup>). Another six animals without any surgical treatments were also included to provide baseline parameters. Blood was drawn from rat tail veins at baseline and at 1, 2, 3, 4, 5, 6, 7, 14, 21, 28 and 35 days. Hematological and clinical chemistry parameters (listed in Table 1) were examined at baseline and at 3, 7, 14, 21, 28 and 35 days. Vector dissemination was evaluated for all blood draw time points. Genomic DNA was isolated from 50  $\mu$ l whole blood using QIAamp DNA Blood Mini kit (Qiagen Inc., Valencia, CA, USA), and quantitative TaqMan PCR was used to determine the copies of Ad-PDGF-B in the bloodstream. The primers used for qPCR bridging the vector backbone and PDGF-B prepro region were as follows: sense, 5'-GGATCTTCGAGTCGACAAGCTT-3'; anti-sense, 5'-ATCTCATAAAGCTCCTCG

GGAAT-3'; and internal fluorogenic probe, 5'-CGC CCAGCAGCGATTCATGGTGAT-3'. The resulting amplicon was detected by ABI Prism 7700 sequence detection instrument (Applied Biosystems, Foster City, CA, USA), and the thermal condition was as follows: 50 °C for 2 min, 95 °C at 10 min followed by 45 cycles of 95 °C for 15 s and 60 °C for 1 min. The assay sensitivity was 30 copies per 500 ng DNA. There was no cross-reaction with Ad vector encoding PDGF-A, PDGF-1308 (dominant-negative, PDGF mutant), bone morphogenetic protein-7, noggin, bone sialoprotein, Ad-Luc or green fluorescent protein.

### Statistical analysis

One-way ANOVA with Tukey test was used to analyze the difference of coded specimens for histomorphometric, BS-SEM, micro-CT, biomechanical and functional parameters between PDGF-treated (collagen containing 0.3 mg ml<sup>-1</sup> rhPDGF-BB, 5.5 × 10<sup>8</sup> or 5.5 × 10<sup>9</sup> pfu ml<sup>-1</sup> Ad-PDGF-B) and non-PDGF-treated (collagen alone) groups at each time point. For evaluating the safety profile, the difference of vector replicates, hematological and chemical parameters between experimental groups (collagen containing 5.5 × 10<sup>8</sup> or 5.5 × 10<sup>9</sup> pfu ml<sup>-1</sup> Ad-PDGF-B) were evaluated for time-dependent dynamics with the control (collagen alone) group using Bonferroni post-tests, and the significance was assessed by repeated-measures ANOVA. The statistical difference was considered with a *P*-value of <0.05.

### Conflict of interest

Lois A Chandler and Barbara Sosnowski are employees of Tissue Repair Company. Steven A Goldstein may receive royalties if distributed by the University of Michigan, and the University of Michigan may benefit from the subject of this paper, as a result of the technology that was licensed to Tissue Repair Company. William Giannobile has financial interest in BioMimetic Therapeutics, Inc.

### Acknowledgements

We thank Valeria Pontelli Navarro Tedeschi for assistance with animal surgeries, Dennis Kayner for assisting removal of the implants, Dr. Noboru Kikuchi for establishing finite element models and Anna Colvig for performing hematological and clinical chemical examinations. This study was supported in part by the grants from the National Institutes of Health (NIH)/National Institute of Dental and Craniofacial Research (NIDCR) (R01-DE13397) and the AO Foundation Research Advisory Council (Davos, Switzerland) to WVG.

### References

- 1 Wikesjo UM, Sorensen RG, Wozney JM. Augmentation of alveolar bone and dental implant osseointegration: clinical implications of studies with rhBMP-2. *J Bone Joint Surg Am* 2001; **83-A** (Suppl 1): S136-S145.
- 2 Lynch SE, de Castilla GR, Williams RC, Kiritsy CP, Howell TH, Reddy MS *et al*. The effects of short-term application of a

- combination of platelet-derived and insulin-like growth factors on periodontal wound healing. *J Periodontol* 1991; **62**: 458-467.
- 3 Fang J, Zhu YY, Smiley E, Bonadio J, Rouleau JP, Goldstein SA *et al*. Stimulation of new bone formation by direct transfer of osteogenic plasmid genes. *Proc Natl Acad Sci USA* 1996; **93**: 5753-5758.
- 4 Ramseier CA, Abramson ZR, Jin Q, Giannobile WV. Gene therapeutics for periodontal regenerative medicine. *Dent Clin North Am* 2006; **50**: 245-263, ix.
- 5 Ghosh SS, Gopinath P, Ramesh A. Adenoviral vectors: a promising tool for gene therapy. *Appl Biochem Biotechnol* 2006; **133**: 9-29.
- 6 Chang PC, Cirelli JA, Jin Q, Seol YJ, Sugai JV, D'Silva NJ *et al*. Adenovirus encoding human platelet-derived growth factor-B delivered to alveolar bone defects exhibits safety and biodistribution profiles favorable for clinical use. *Hum Gene Ther* 2009; **20**: 486-496.
- 7 Gu DL, Nguyen T, Gonzalez AM, Printz MA, Pierce GF, Sosnowski BA *et al*. Adenovirus encoding human platelet-derived growth factor-B delivered in collagen exhibits safety, biodistribution, and immunogenicity profiles favorable for clinical use. *Mol Ther* 2004; **9**: 699-711.
- 8 Barrientos S, Stojadinovic O, Golinko MS, Brem H, Tomic-Canic M. Growth factors and cytokines in wound healing. *Wound Repair Regen* 2008; **16**: 585-601.
- 9 Anusaksathien O, Jin Q, Zhao M, Somerman MJ, Giannobile WV. Effect of sustained gene delivery of platelet-derived growth factor or its antagonist (PDGF-1308) on tissue-engineered cementum. *J Periodontol* 2004; **75**: 429-440.
- 10 Canalis E, McCarthy TL, Centrella M. Effects of platelet-derived growth factor on bone formation *in vitro*. *J Cell Physiol* 1989; **140**: 530-537.
- 11 Nevins M, Giannobile WV, McGuire MK, Kao RT, Mellonig JT, Hinrichs JE *et al*. Platelet-derived growth factor stimulates bone fill and rate of attachment level gain: results of a large multicenter randomized controlled trial. *J Periodontol* 2005; **76**: 2205-2215.
- 12 Uhl E, Rosken F, Sirsjo A, Messmer K. Influence of platelet-derived growth factor on microcirculation during normal and impaired wound healing. *Wound Repair Regen* 2003; **11**: 361-367.
- 13 Simion M, Rocchietta I, Monforte M, Maschera E. Three-dimensional alveolar bone reconstruction with a combination of recombinant human platelet-derived growth factor BB and guided bone regeneration: a case report. *Int J Periodontics Restorative Dent* 2008; **28**: 239-243.
- 14 Jin Q, Anusaksathien O, Webb SA, Printz MA, Giannobile WV. Engineering of tooth-supporting structures by delivery of PDGF gene therapy vectors. *Mol Ther* 2004; **9**: 519-526.
- 15 Chang PC, Seol YJ, Kikuchi N, Goldstein SA, Giannobile WV. Functional apparent moduli: Indicators to predict dynamics of oral implant osseointegration (in review).
- 16 Gabet Y, Müller R, Levy J, Dimarchi R, Chorev M, Bab I *et al*. Parathyroid hormone 1-34 enhances titanium implant anchorage in low-density trabecular bone: a correlative micro-computed tomographic and biomechanical analysis. *Bone* 2006; **39**: 276-282.
- 17 Ramp LC, Jeffcoat RL. Dynamic behavior of implants as a measure of osseointegration. *Int J Oral Maxillofac Implants* 2001; **16**: 637-645.
- 18 Lin Z, Sugai JV, Jin Q, Chandler LA, Giannobile WV. Platelet-derived growth factor-B gene delivery sustains gingival fibroblast signal transduction. *J Periodontol Res* 2008; **43**: 440-449.
- 19 De Donatis A, Comito G, Buricchi F, Vinci MC, Parenti A, Caselli A *et al*. Proliferation versus migration in platelet-derived growth factor signaling: the key role of endocytosis. *J Biol Chem* 2008; **283**: 19948-19956.

- 20 Hsieh SC, Graves DT. Pulse application of platelet-derived growth factor enhances formation of a mineralizing matrix while continuous application is inhibitory. *J Cell Biochem* 1998; **69**: 169–180.
- 21 Tokunaga A, Oya T, Ishii Y, Motomura H, Nakamura C, Ishizawa S *et al*. PDGF receptor beta is a potent regulator of mesenchymal stromal cell function. *J Bone Miner Res* 2008; **23**: 1519–1528.
- 22 Kono SJ, Oshima Y, Hoshi K, Bonewald LF, Oda H, Nakamura K *et al*. Erk pathways negatively regulate matrix mineralization. *Bone* 2007; **40**: 68–74.
- 23 Huang Z, Nelson ER, Smith RL, Goodman SB. The sequential expression profiles of growth factors from osteoprogenitors (correction of osteoprogenitors) to osteoblasts *in vitro*. *Tissue Eng* 2007; **13**: 2311–2320.
- 24 Ng F, Boucher S, Koh S, Sastry KS, Chase L, Lakshminpathy U *et al*. PDGF, TGF-beta, and FGF signaling is important for differentiation and growth of mesenchymal stem cells (MSCs): transcriptional profiling can identify markers and signaling pathways important in differentiation of MSCs into adipogenic, chondrogenic, and osteogenic lineages. *Blood* 2008; **112**: 295–307.
- 25 Kratchmarova I, Blagoev B, Haack-Sorensen M, Kassem M, Mann M. Mechanism of divergent growth factor effects in mesenchymal stem cell differentiation. *Science* 2005; **308**: 1472–1477.
- 26 Doukas J, Chandler LA, Gonzalez AM, Gu D, Hoganson DK, Ma C *et al*. Matrix immobilization enhances the tissue repair activity of growth factor gene therapy vectors. *Hum Gene Ther* 2001; **12**: 783–798.
- 27 Pouton CW, Wagstaff KM, Roth DM, Moseley GW, Jans DA. Targeted delivery to the nucleus. *Adv Drug Deliv Rev* 2007; **59**: 698–717.
- 28 Dunn CA, Jin Q, Taba Jr M, Franceschi RT, Bruce Rutherford R, Giannobile WV. BMP gene delivery for alveolar bone engineering at dental implant defects. *Mol Ther* 2005; **11**: 294–299.
- 29 Andrae J, Gallini R, Betsholtz C. Role of platelet-derived growth factors in physiology and medicine. *Genes Dev* 2008; **22**: 1276–1312.
- 30 Tokuda H, Takai S, Hanai Y, Harada A, Matsushima-Nishiwaki R, Kato H *et al*. Potentiation by platelet-derived growth factor-BB of FGF-2-stimulated VEGF release in osteoblasts. *J Bone Miner Metab* 2008; **26**: 335–341.
- 31 Zhang J, Cao R, Zhang Y, Jia T, Cao Y, Wahlberg E. Differential roles of PDGFR-[alpha] and PDGFR-[beta] in angiogenesis and vessel stability. *FASEB J* 2008; **23**: 153–163.
- 32 Douglas JT. Adenoviral vectors for gene therapy. *Mol Biotechnol* 2007; **36**: 71–80.
- 33 Hartman ZC, Appledorn DM, Amalfitano A. Adenovirus vector induced innate immune responses: impact upon efficacy and toxicity in gene therapy and vaccine applications. *Virus Res* 2008; **132**: 1–14.
- 34 Sonobe J, Okubo Y, Kaihara S, Miyatake S, Bessho K. Osteoinduction by bone morphogenetic protein 2-expressing adenoviral vector: application of biomaterial to mask the host immune response. *Hum Gene Ther* 2004; **15**: 659–668.
- 35 Wang Y, Yang Z, Liu S, Kon T, Krol A, Li CY *et al*. Characterisation of systemic dissemination of nonreplicating adenoviral vectors from tumours in local gene delivery. *Br J Cancer* 2005; **92**: 1414–1420.
- 36 Paleos CM, Tziveleka LA, Sideratou Z, Tsiourvas D. Gene delivery using functional dendritic polymers. *Expert Opin Drug Deliv* 2009; **6**: 27–38.
- 37 Ditto AJ, Shah PN, Gump LR, Yun YH. Nanospheres formulated from l-tyrosine polyphosphate exhibiting sustained release of polyplexes and *in vitro* controlled transfection properties. *Mol Pharm* 2009; **6**: 986–995.
- 38 Traini T, Degidi M, Iezzi G, Artese L, Piattelli A. Comparative evaluation of the peri-implant bone tissue mineral density around unloaded titanium dental implants. *J Dent* 2007; **35**: 84–92.
- 39 Otsu N. Threshold selection method from gray-level histograms. *IEEE Trans Syst Man Cybern* 1979; **9**: 62–66.

Supplementary Information accompanies the paper on Gene Therapy website (<http://www.nature.com/gt>)

## REFERENCES

1. WinterGreen Research, I. Worldwide Nanotechnology Dental Implant Market Shares, Strategies, and Forecasts, 2009 to 2015. 2009.
2. Schwartz, N. L., Whitsett, L. D., Berry, T. G., and Stewart, J. L. Unserviceable crowns and fixed partial dentures: life-span and causes for loss of serviceability. *J Am Dent Assoc*, *81*: 1395-1401, 1970.
3. Carr, A. B. and Laney, W. R. Maximum occlusal force levels in patients with osseointegrated oral implant prostheses and patients with complete dentures. *Int J Oral Maxillofac Implants*, *2*: 101-108, 1987.
4. Carlsson, G. E., Lindquist, L. W., and Jemt, T. Long-term marginal periimplant bone loss in edentulous patients. *Int J Prosthodont*, *13*: 295-302, 2000.
5. Schropp, L., Wenzel, A., Kostopoulos, L., and Karring, T. Bone healing and soft tissue contour changes following single-tooth extraction: a clinical and radiographic 12-month prospective study. *Int J Periodontics Restorative Dent*, *23*: 313-323, 2003.
6. Buser, D., Martin, W., and Belser, U. C. Optimizing esthetics for implant restorations in the anterior maxilla: anatomic and surgical considerations. *Int J Oral Maxillofac Implants*, *19 Suppl*: 43-61, 2004.
7. Hammerle, C. H. and Glauser, R. Clinical evaluation of dental implant treatment. *Periodontol 2000*, *34*: 230-239, 2004.
8. Becker, W., Lynch, S. E., Lekholm, U., Becker, B. E., Caffesse, R., Donath, K., and Sanchez, R. A comparison of ePTFE membranes alone or in combination with platelet-derived growth factors and insulin-like growth factor-I or demineralized

- freeze-dried bone in promoting bone formation around immediate extraction socket implants. *J Periodontol*, 63: 929-940, 1992.
9. Giannobile, W. V., Finkelman, R. D., and Lynch, S. E. Comparison of canine and non-human primate animal models for periodontal regenerative therapy: results following a single administration of PDGF/IGF-I. *J Periodontol*, 65: 1158-1168, 1994.
  10. Giannobile, W. V., Hernandez, R. A., Finkelman, R. D., Ryan, S., Kiritsy, C. P., D'Andrea, M., and Lynch, S. E. Comparative effects of platelet-derived growth factor-BB and insulin-like growth factor-I, individually and in combination, on periodontal regeneration in *Macaca fascicularis*. *J Periodontal Res*, 31: 301-312, 1996.
  11. Park, J. B., Matsuura, M., Han, K. Y., Norderyd, O., Lin, W. L., Genco, R. J., and Cho, M. I. Periodontal regeneration in class III furcation defects of beagle dogs using guided tissue regenerative therapy with platelet-derived growth factor. *J Periodontol*, 66: 462-477, 1995.
  12. Rutherford, R. B., Niekrash, C. E., Kennedy, J. E., and Charette, M. F. Platelet-derived and insulin-like growth factors stimulate regeneration of periodontal attachment in monkeys. *J Periodontal Res*, 27: 285-290, 1992.
  13. Howell, T. H., Fiorellini, J. P., Paquette, D. W., Offenbacher, S., Giannobile, W. V., and Lynch, S. E. A phase I/II clinical trial to evaluate a combination of recombinant human platelet-derived growth factor-BB and recombinant human insulin-like growth factor-I in patients with periodontal disease. *J Periodontol*, 68: 1186-1193, 1997.
  14. Nevins, M., Giannobile, W. V., McGuire, M. K., Kao, R. T., Mellonig, J. T., Hinrichs, J. E., McAllister, B. S., Murphy, K. S., McClain, P. K., Nevins, M. L., Paquette, D. W., Han, T. J., Reddy, M. S., Lavin, P. T., Genco, R. J., and Lynch, S. E. Platelet-derived growth factor

- stimulates bone fill and rate of attachment level gain: results of a large multicenter randomized controlled trial. *J Periodontol*, 76: 2205-2215, 2005.
15. Anusaksathien, O. and Giannobile, W. V. Growth factor delivery to re-engineer periodontal tissues. *Curr Pharm Biotechnol*, 3: 129-139, 2002.
  16. Bonadio, J. Tissue engineering via local gene delivery: update and future prospects for enhancing the technology. *Adv Drug Deliv Rev*, 44: 185-194, 2000.
  17. Boyne, P. J., Marx, R. E., Nevins, M., Triplett, G., Lazaro, E., Lilly, L. C., Alder, M., and Nummikoski, P. A feasibility study evaluating rhBMP-2/absorbable collagen sponge for maxillary sinus floor augmentation. *Int J Periodontics Restorative Dent*, 17: 11-25, 1997.
  18. Cochran, D. L., Jones, A. A., Lilly, L. C., Fiorellini, J. P., and Howell, H. Evaluation of recombinant human bone morphogenetic protein-2 in oral applications including the use of endosseous implants: 3-year results of a pilot study in humans. *J Periodontol*, 71: 1241-1257, 2000.
  19. van den Bergh, J. P., ten Bruggenkate, C. M., Groeneveld, H. H., Burger, E. H., and Tuinzing, D. B. Recombinant human bone morphogenetic protein-7 in maxillary sinus floor elevation surgery in 3 patients compared to autogenous bone grafts. A clinical pilot study. *J Clin Periodontol*, 27: 627-636, 2000.
  20. Terrell, T. G., Working, P. K., Chow, C. P., and Green, J. D. Pathology of recombinant human transforming growth factor-beta 1 in rats and rabbits. *Int Rev Exp Pathol*, 34 Pt B: 43-67, 1993.
  21. Langer, R. Drug delivery and targeting. *Nature*, 392: 5-10, 1998.

22. Murphy, K. G. and Gunsolley, J. C. Guided tissue regeneration for the treatment of periodontal intrabony and furcation defects. A systematic review. *Ann Periodontol*, 8: 266-302, 2003.
23. Reynolds, M. A., Aichelmann-Reidy, M. E., Branch-Mays, G. L., and Gunsolley, J. C. The efficacy of bone replacement grafts in the treatment of periodontal osseous defects. A systematic review. *Ann Periodontol*, 8: 227-265, 2003.
24. Jin, Q., Anusaksathien, O., Webb, S. A., Printz, M. A., and Giannobile, W. V. Engineering of tooth-supporting structures by delivery of PDGF gene therapy vectors. *Mol Ther*, 9: 519-526, 2004.
25. Dunn, C. A., Jin, Q., Taba, M., Jr., Franceschi, R. T., Bruce Rutherford, R., and Giannobile, W. V. BMP gene delivery for alveolar bone engineering at dental implant defects. *Mol Ther*, 11: 294-299, 2005.
26. Gu, D. L., Nguyen, T., Gonzalez, A. M., Printz, M. A., Pierce, G. F., Sosnowski, B. A., Phillips, M. L., and Chandler, L. A. Adenovirus encoding human platelet-derived growth factor-B delivered in collagen exhibits safety, biodistribution, and immunogenicity profiles favorable for clinical use. *Mol Ther*, 9: 699-711, 2004.
27. Ostman, A. and Heldin, C. H. Involvement of platelet-derived growth factor in disease: development of specific antagonists. *Adv Cancer Res*, 80: 1-38, 2001.
28. Kaplan, D. R., Chao, F. C., Stiles, C. D., Antoniades, H. N., and Scher, C. D. Platelet alpha granules contain a growth factor for fibroblasts. *Blood*, 53: 1043-1052, 1979.
29. Seppa, H., Grotendorst, G., Seppa, S., Schiffmann, E., and Martin, G. R. Platelet-derived growth factor in chemotactic for fibroblasts. *J Cell Biol*, 92: 584-588, 1982.

30. Heldin, P., Laurent, T. C., and Heldin, C. H. Effect of growth factors on hyaluronan synthesis in cultured human fibroblasts. *Biochem J*, 258: 919-922, 1989.
31. Rosenkranz, S. and Kazlauskas, A. Evidence for distinct signaling properties and biological responses induced by the PDGF receptor alpha and beta subtypes. *Growth Factors*, 16: 201-216, 1999.
32. Heldin, C. H., Ostman, A., and Ronnstrand, L. Signal transduction via platelet-derived growth factor receptors. *Biochim Biophys Acta*, 1378: F79-113, 1998.
33. Kaminski, W. E., Lindahl, P., Lin, N. L., Broudy, V. C., Crosby, J. R., Hellstrom, M., Swolin, B., Bowen-Pope, D. F., Martin, P. J., Ross, R., Betsholtz, C., and Raines, E. W. Basis of hematopoietic defects in platelet-derived growth factor (PDGF)-B and PDGF beta-receptor null mice. *Blood*, 97: 1990-1998, 2001.
34. Parkar, M. H., Kuru, L., Giouzei, M., and Olsen, I. Expression of growth-factor receptors in normal and regenerating human periodontal cells. *Arch Oral Biol*, 46: 275-284, 2001.
35. Green, R. J., Usui, M. L., Hart, C. E., Ammons, W. F., and Narayanan, A. S. Immunolocalization of platelet-derived growth factor A and B chains and PDGF-alpha and beta receptors in human gingival wounds. *J Periodontal Res*, 32: 209-214, 1997.
36. Nishimura, F. and Terranova, V. P. Comparative study of the chemotactic responses of periodontal ligament cells and gingival fibroblasts to polypeptide growth factors. *J Dent Res*, 75: 986-992, 1996.
37. Oates, T. W., Rouse, C. A., and Cochran, D. L. Mitogenic effects of growth factors on human periodontal ligament cells in vitro. *J Periodontol*, 64: 142-148, 1993.

38. Haase, H. R., Clarkson, R. W., Waters, M. J., and Bartold, P. M. Growth factor modulation of mitogenic responses and proteoglycan synthesis by human periodontal fibroblasts. *J Cell Physiol*, *174*: 353-361, 1998.
39. Matsuda, N., Lin, W. L., Kumar, N. M., Cho, M. I., and Genco, R. J. Mitogenic, chemotactic, and synthetic responses of rat periodontal ligament fibroblastic cells to polypeptide growth factors in vitro. *J Periodontol*, *63*: 515-525, 1992.
40. Zaman, K. U., Sugaya, T., and Kato, H. Effect of recombinant human platelet-derived growth factor-BB and bone morphogenetic protein-2 application to demineralized dentin on early periodontal ligament cell response. *J Periodont Res*, *34*: 244-250, 1999.
41. Lynch, S. E., de Castilla, G. R., Williams, R. C., Kiritsy, C. P., Howell, T. H., Reddy, M. S., and Antoniades, H. N. The effects of short-term application of a combination of platelet-derived and insulin-like growth factors on periodontal wound healing. *J Periodontol.*, *62*: 458-467, 1991.
42. Camelo, M., Nevins, M. L., Schenk, R. K., Lynch, S. E., and Nevins, M. Periodontal regeneration in human Class II furcations using purified recombinant human platelet-derived growth factor-BB (rhPDGF-BB) with bone allograft. *Int J Periodontics Restorative Dent*, *23*: 213-225, 2003.
43. Steed, D. L. Clinical evaluation of recombinant human platelet-derived growth factor for the treatment of lower extremity ulcers. *Plast Reconstr Surg*, *117*: 143S-149S; discussion 150S-151S, 2006.
44. Cooke, J. W., Sarment, D. P., Whitesman, L. A., Miller, S. E., Jin, Q., Lynch, S. E., and Giannobile, W. V. Effect of rhPDGF-BB delivery on mediators of periodontal wound repair. *Tissue Eng*, *12*: 1441-1450, 2006.

45. Sarment, D. P., Cooke, J. W., Miller, S. E., Jin, Q., McGuire, M. K., Kao, R. T., McClain, P. K., McAllister, B. S., Lynch, S. E., and Giannobile, W. V. Effect of rhPDGF-BB on bone turnover during periodontal repair. *J Clin Periodontol*, 33: 135-140, 2006.
46. Giannobile, W. V., Lee, C. S., Tomala, M. P., Tejada, K. M., and Zhu, Z. Platelet-derived growth factor (PDGF) gene delivery for application in periodontal tissue engineering. *J Periodontol*, 72: 815-823, 2001.
47. Zhu, Z., Lee, C. S., Tejada, K. M., and Giannobile, W. V. Gene transfer and expression of platelet-derived growth factors modulate periodontal cellular activity. *J Dent Res*, 80: 892-897, 2001.
48. Anusaksathien, O., Webb, S. A., Jin, Q. M., and Giannobile, W. V. Platelet-derived growth factor gene delivery stimulates *ex vivo* gingival repair. *Tissue Eng*, 9: 745-756, 2003.
49. Jin, Q. M., Anusaksathien, O., Webb, S. A., Rutherford, R. B., and Giannobile, W. V. Gene therapy of bone morphogenetic protein for periodontal tissue engineering. *J Periodontol*, 74: 202-213, 2003.
50. Traini, T., Degidi, M., Iezzi, G., Artese, L., and Piattelli, A. Comparative evaluation of the peri-implant bone tissue mineral density around unloaded titanium dental implants. *J Dent*, 35: 84-92, 2007.
51. Otsu, N. A threshold selection method from gray-level histograms. *IEEE Trans. Sys., Man., Cyber.*, 9: 62-66, 1979.